Thermal Performance of Exterior Insulation and Finish Systems Containing Vacuum Insulation Panels

Kenneth Childs

Therese Stovall
Member ASHRAE

Kaushik Biswas
Associate Member ASHRAE

Lawrence D. Carbary

ABSTRACT

A high-performance wall system is under development to improve wall thermal performance to a level of U-factor of 0.19 W/(m^2·K) (R-30 [h·ft^2·F]/Btu) in a standard wall thickness by incorporating vacuum insulation panels (VIPs) into an exterior insulation finish system (EIFS). Such a system would be applicable to new construction and will offer a solution to more challenging retrofit situations as well. Multiple design options were considered to balance the need to protect the VIPs during construction and building operation, while minimizing heat transfer through the wall system. The results reported here encompass an in-depth assessment of potential system performances including thermal modeling, detailed laboratory measurements under controlled conditions on the component, and system levels according to ASTM C518 (ASTM 2010). The results demonstrate the importance of maximizing the VIP coverage over the wall face. The results also reveal the impact of both the design and execution of system details, such as the joints between adjacent VIPs. The test results include an explicit modeled evaluation of the system performance in a clear wall.

INTRODUCTION

According to the US Department of Energy, buildings in the commercial and residential environment use 40% of the energy consumed in the US (DOE 2008). The global awareness of excessive energy use and the resulting emissions of carbon dioxide have created an environment where businesses and individuals alike are striving for reduced energy consumption. Building codes around the world continue to require reduced energy use of commercial and residential structures.

This paper focuses on increasing the insulating value of walls without increasing the thickness. Structures that reach a passive-house wall-construction standard of a U-factor of 0.15 W/(m^2·K) (R-38 [h·ft^2·°F]/Btu) have extremely thick walls when using conventional insulation (Wikipedia 2010). Thick walls result in additional construction detailing of the fenestration components along with eaves and overhangs. The design of an increased insulating wall system without increased thickness is the goal of this paper. Incorporation of superinsulating fumed-silica vacuum insulation panels (VIPs) into expanded polystyrene (EPS) units will allow an increased efficiency system to be installed in the typical exterior insulation-finishing system (EIFS) construction wall system.

DESCRIPTION OF VIP

The VIP is a superinsulating product consisting of a core material vacuum-packaged in a barrier envelope, Figure 1. The performance and life expectancy of the VIP depends on the conductivity and stability of the core material as well as the level of vacuum maintained in service. These products have been used commercially in appliances and shipping containers for many years. While VIP technology is not new, the products have had limited application in the construction industry due in large part to concerns for the limited service life and fragility of the vacuum-packaging system. The combination of paying attention to VIP panel protection by incorporation into a workable and user-friendly system has shown promise for greatly extended service life, suitable for consideration in construction

Lawrence D. Carbary is an Industry Scientist, Dow Corning Corporation, Midland MI, Kaushik Biswas is an R&D Associate, Kenneth Childs is a Senior Scientist, and Therese Stovall is a Distinguished Research Engineer, Retired, Oak Ridge National Laboratory, Oak Ridge, TN.

applications. Although new product and manufacturing process innovations will be required to incorporate this form of insulation into EIFS, the technology can be customized using new adhesive and barrier technologies.

This project documents the steps to evaluate and develop the feasibility of incorporating more highly-insulated materials (VIP) into a standard overall insulation thickness of 75 mm (3 in.) of insulating materials, ultimately removing marketing barriers to the use of EIFS on current buildings that desire high-insulation walls but are limited with current technology/materials.

EXTERIOR INSULATING AND FINISH SYSTEMS (EIFS)

Current insulation materials in the marketplace are limited to material R-0.6–0.9 $m^2 \cdot K/W$ (3.5–5 $h \cdot ft^2 \cdot °F/Btu$) and would require thicknesses of 200–275 mm (8–11 in.) to achieve a U-factor of 0.14 $W/m^2 \cdot K$ (R-40 $h \cdot ft^2 \cdot °F/Btu$). This creates significant implementation issues in both new and retrofit construction. The thickness required using existing materials poses a major barrier to retrofit applications because windows, doors, roofs, and other building details are not designed to accommodate such a drastic change in envelope thickness. Existing forms of EIFSs siding using an average of 50 mm (2 in.) thickness of EPS insulation are already sold today; however, these systems only deliver an average U-factor of 0.3 $W/m^2 \cdot K$ (R-12.9 $h \cdot ft^2 \cdot °F/Btu$).

A new form of insulation made using VIP technology encapsulated into EPS was studied and is expected to achieve 0.14 $W/m^2 \cdot K$ (R-40 $h \cdot ft^2 \cdot °F/Btu$) values with a much smaller thickness.

Higher values of insulation in building envelopes can be achieved with currently available building practices; however, the techniques are not widely used because they either significantly increase the cost of construction or they result in a reduction of the living space available. Current solutions to increase the energy efficiency of building envelopes do exist for retrofit applications; however, these solutions require the use of multiple components such as EPS insulation and siding. In addition to increased labor costs to install the multiple components associated with these solutions, they are also limited in their introduction because EPS insulation can only achieve a limited improvement in thermal resistance.

To enable 0.14 $W/m^2 \cdot K$ (R-40 $h \cdot ft^2 \cdot °F/Btu$) envelope construction, a minimum thickness of 250 mm (10 in.) of EPS foam would be required and this is technically and economically unfeasible in retrofit construction due to the high labor costs required, the poor aesthetics, and the technical capability of the solution. A solution to this is the incorporation of vacuum-insulated panel insulation into a significantly improved form of EIFS to increase the U-factor of a typical wall from 0.3 $W/m^2 \cdot K$ to 0.14 $W/m^2 \cdot K$ (R-12.9 $h \cdot ft^2 \cdot °F/Btu$ to R-40 $h \cdot ft^2 \cdot °F/Btu$). While EIFSs outperform most cladding systems, this new system creates significant performance improvements in terms of increased thermal resistance per dimension of thickness of insulation delivered versus current envelope systems.

A cross section of typical EIFSs using EPS as the insulation is shown in Figure 2. EIFSs offers four distinct advantages: any desired thickness of the insulation can be used to achieve higher insulation walls, incorporates an integral air barrier component, completion of the exterior with minimal interior disruption, and minimal thermal bridging. The technology is so versatile that it is possible to prefabricate the insulated panels in a fabrication plant and assemble them at the construction site. This not only speeds up the construction process, but minimizes the impact of climatic conditions on the construction. As it stands today, EIFS technology is both versatile and cost-effective. By integrating VIP panels into EIFSs, a new capability is brought to the construction market that helps new or existing buildings achieve close to zero

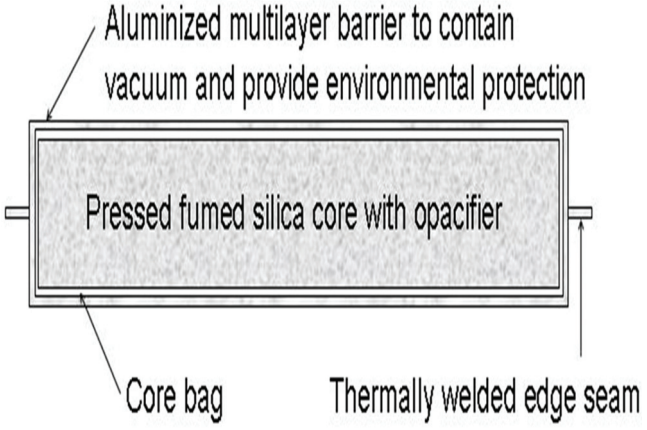

Figure 1 *Cross section of VIP.*

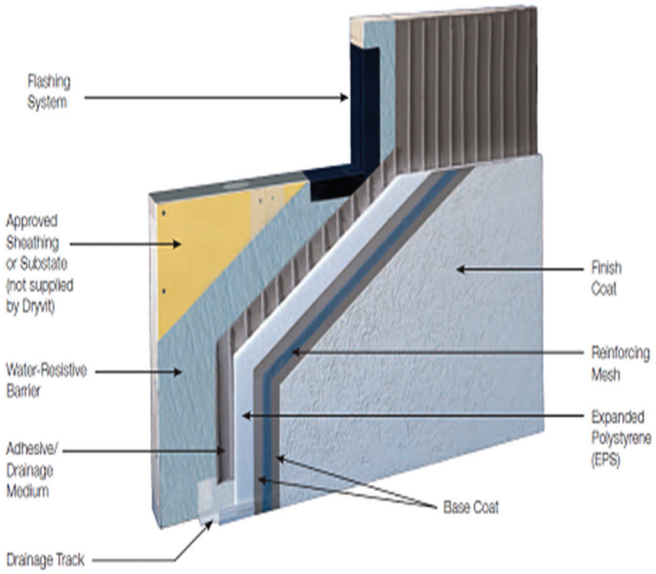

Figure 2 *Example of EIFS.*

energy levels through a superinsulating exterior system, ultimately helping to minimize the energy needs of these buildings.

There are three general classes of core materials that can be considered for use in VIP: polymeric foams; fiberglass; and nanoporous silica. The first two are characterized by cell/pore sizes in excess of 5 μm, whereas the pore size of nanoporous silica has a pore size on the 50 nm (0.05 μm) range or 100 times smaller. The larger pore size of foams and fiberglass means that the vacuum panel pressure must be maintained at ~100 times lower absolute pressure level than a nanoporous silica panel for the same thermal performance. The change in thermal conductivity for the three types of cores is illustrated in Figure 3.

For construction applications, the normal range of ambient water vapor partial pressure (even at 100% rh) is limited and on the order of tens of millibar. Water vapor permeates through barrier films much faster than other atmospheric gases due to the molecular size. For a silica VIP, this pressure of 10–30 mbar only causes a minor loss in thermal performance; whereas, for foam and fiberglass VIP applications have decreased their insulating value significantly.

Older generations of VIP insulation failed to offer long-term performance due to the fact that organic chemical materials were used in the VIP products. These organic materials tended to lose mass due to the loss of vapor over time and this resulted in reduced performance. Vapor loss within the vacuum system will elevate the internal pressure resulting in reduced thermal performance. The form of VIP insulation described here is made from an inorganic silica (silicon dioxide) chemistry which is inert and will not change over time. Long-term aging studies of this material suggest that it will offer effective performance over a 25+ year period (Wegger et al. 2011).

The current drawback associated with all forms of VIP insulation is the fact that the insulation value is significantly decreased if the insulation panel loses its vacuum seal due to a puncture or rupture. While this can be a significant drawback in construction applications that involve nailing and fastening, it is possible to overcome with innovative design techniques such as encapsulating the VIPs into rigid boards and adhesively fastening them to a building structure. It is critical to have nonhazardous, long-lasting safe adhesives for the attachment of VIP panels. Adhesives with very low shrinkage, such as neutral curing silicone materials, are needed so that the curing process will not compromise the foil bag. The adhesive and VIP systems have to be able to resist the windloads and gravity loads associated with the construction application and should be tested to industry standards for such applications.

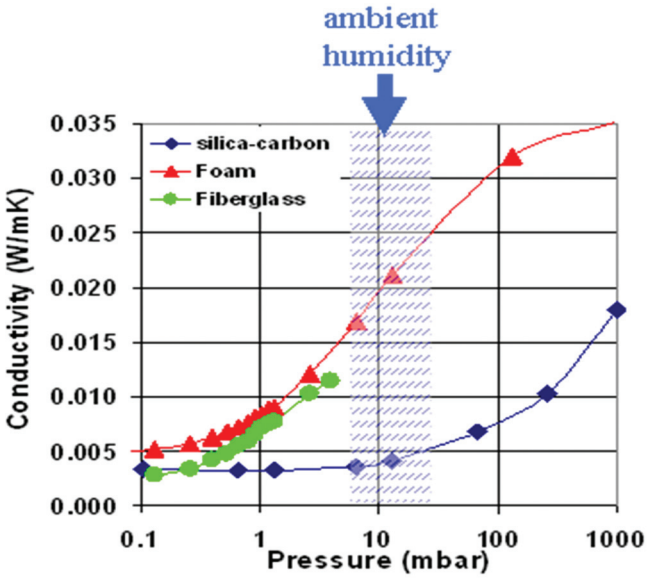

Figure 3 *Change in thermal performance of VIP during loss of pressure when using different core materials.*

MEASUREMENT METHODOLOGY

The heat flux meter (HFM) apparatus is a secondary measurement method, often used to evaluate the thermal conductivity of homogenous materials. The typical construction and use are described in ASTM C518 (ASTM 2010). The two plates, shown in Figure 4, are carefully controlled at fixed temperatures. As the heat flows from the hot plate and through the test specimen into the cold plate, a small temperature difference across the transducers generates an electrical signal that is proportional to the heat flux through the transducer. For homogenous specimens with uniform plate temperatures, the heat flux is unidirectional and can therefore be used with Fourier's Law to calculate the thermal conductivity of the material.

Most HFM apparatus use a single transducer on each of the temperature-controlled plates. A special-purpose apparatus has been designed to facilitate the characterization of nonhomogenous specimens. This apparatus has an array of transducers on both the top and bottom plates, so that nonuniform heat flux patterns can be measured. The design of this array is shown in Figure 5. The test produces a map of heat transfer over this collection of thirty (15 top and 15 bottom)

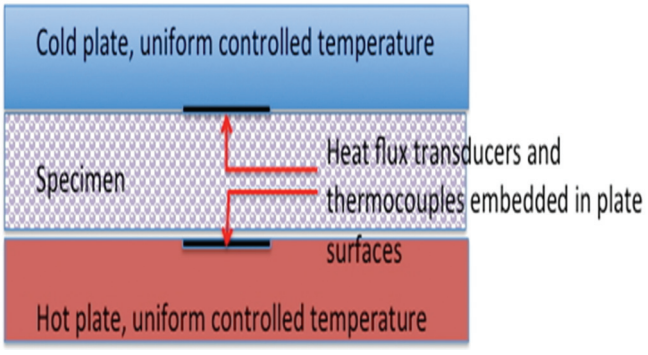

Figure 4 *Conceptual cross section of a HFM apparatus.*

7.5 × 7.5 cm (3 × 3 in.) transducers. Even with this extensive measurement scheme, it is typically necessary to merge the test measurements with a mathematical model to fully characterize complex specimens. This apparatus has previously been used to examine VIPs as a part of a refrigerator design project (Wilkes et al. 1997; Wilkes et al. 1999; Stovall and Brzezinski 2002).

A nonstandard calibration method, similar to that described in ASTM C1667, was used for this project to more accurately measure very small heat flux values (ASTM 2009). The calibration process, along with other test practice details, are not described here. Using this calibration process, the heat flux values reported here have an extended combined uncertainty between 5% and 10% at a 95% confidence level, with the greater uncertainty corresponding to the lower heat flux values found over the center of a VIP (Taylor and Kuyatt 1994).

DESCRIPTION OF SPECIMENS TESTED

In order to use VIPs in a building, it is necessary to protect them from puncture and abrasion during the construction process. In the proposed designs, that is accomplished by encasing the vacuum panels within closed-cell foam insulation. Within this general design framework, there are a large number of possible permutations with regard to: the arrangement of panel seams relative to joints where panels are adjacent to each other, the type of foam insulation, the thickness of the foam separation between VIPs, and other possible protective materials.

Ten special purpose test specimens were prepared to place these variations within the monitored area of the HFM apparatus. Figure 6 demonstrates how these test specimens are representative of panel intersections within a full wall. The joints between VIPs in the test specimens were located along the lines of central transducers. All of the assemblies cover an area slightly less than 610 × 610 mm (24 × 24 in.) and consist of a layer containing 2.5 cm (1 in.) thick VIPs sandwiched between layers of rigid foam insulation, either EPS or extruded polystyrene (XPS). The assemblies differ in (1) the number and size of VIPs they contain (one large panel, two half panels, or one half panel with two quarter panels), (2) the type and thickness of the rigid foam insulation layers, and (3) the material adjacent to the edges of the VIPs. An example of an assembly construction is illustrated in the exploded view of design option 1 shown in Figure 7. A summary of the key features of the VIPs tested is given in Table 1. Some internal details of design options 11 and 12 could not be determined by visual examination of the assemblies.

In addition to the above VIP assemblies, tests were also performed on two bare VIPs that were approximately 59.6 cm^2 (23.5 in^2). The thermal conductivity of EPS and XPS foam boards similar to those used in the assemblies was measured.

TEST DATA

Each of the assemblies contains EPS insulation board, XPS insulation board, or a combination of both. Since the conductivity of these materials influences the performance of the assemblies, a series of HFM apparatus tests were performed to determine the thermal conductivity of both EPS and XPS as a function of temperature. The temperature-dependent thermal conductivity of EPS and XPS from these measurements is given by Equations 1 and 2, respectively, and shown in Figure 8.

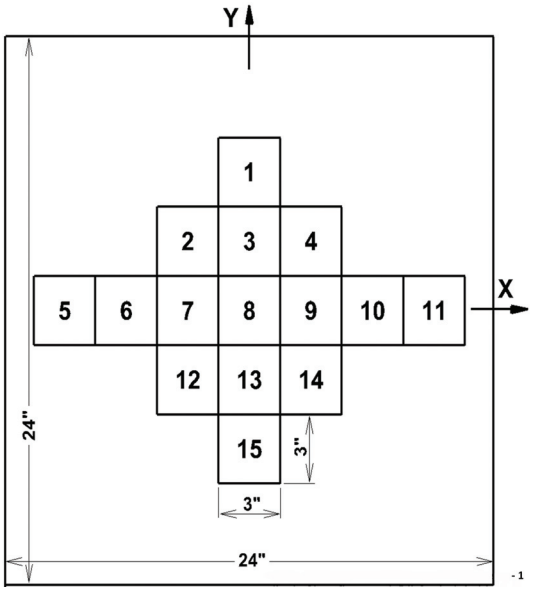

Figure 5 *HFT numbering scheme: 1 (back of HFM), 5 (left edge), 11 (right edge), 15 (front).*

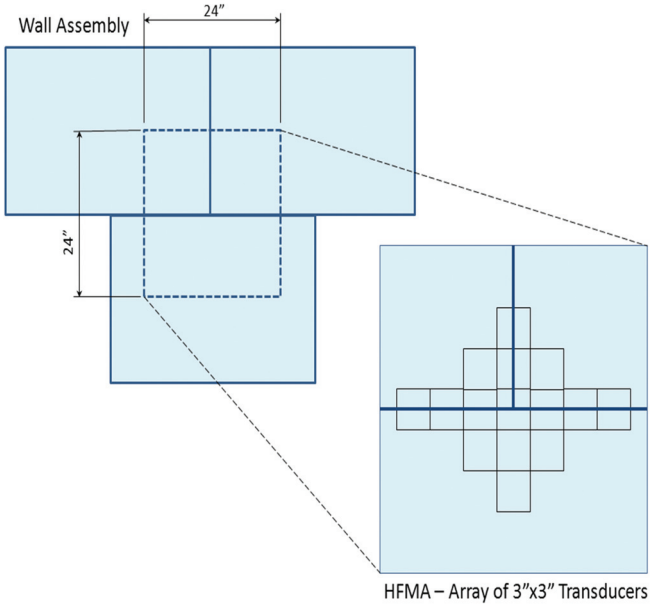

Figure 6 *Test specimen represents joints between panels on a full wall.*

$$k = 3.4020 \times 10^{-2} + 1.4591 \times 10^{-4} T \quad (1)$$

$$k = 2.5638 \times 10^{-2} + 1.1688 \times 10^{-4} T \quad (2)$$

where

T = temperature, °C

K = thermal conductivity, W/m·K.

In the series of the tests performed on the ten VIP assemblies and the two large individual VIPs, the bottom-plate temperature is set to 35°C and the top-plate temperature is set to 12.78°C. Some of the specimens were measured multiple times. The following pages give the measured fluxes from a representative test for each of the specimens. Figures 9, 11, 13, 15, 17, 19, 21, 23, 25, and 27 give the measured flux (W/m^2) for each heat flux transducer (HFT) location. The top number for each location is the flux on the upper surface, and the bottom number is the flux on the lower surface. Note that HFT 12 on the bottom plate is inoperable, and HFT 11 on the upper plate operates only intermittently. To aid in interpreting the fluxes, the location of each VIP in the assembly is also outlined in the figure. The white space represents the material surrounding the VIPs. At the bottom of each page are two plots of the heat fluxes along the two centerlines of the transducer array. These are Figures 10, 12, 14, 16, 18, 20, 22, 24, 26, and 28. Uncertainty bounds of 7.5% are shown on these plots.

Look at these results for design option 1 in Figure 9 and Figure 10. As you travel across the *x*-axis from left to right, you see the flux is slightly greater near the edges, but the greatest

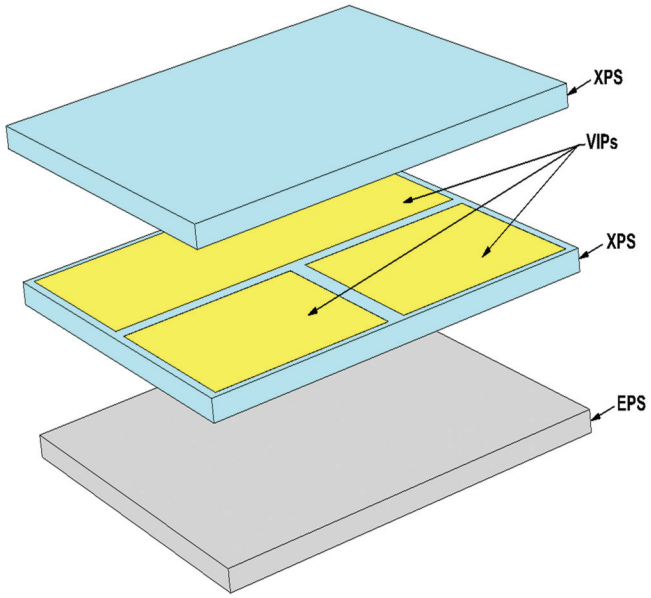

Figure 7 *Exploded view of design option 1.*

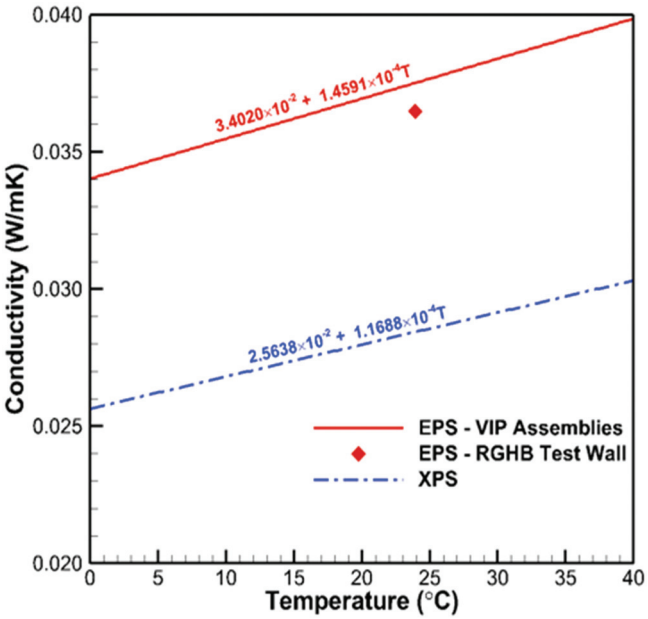

Figure 8 *Foam board thermal conductivity.*

Table 1. Test Specimen Construction Details

Design Option	Number VIPs	Material Surrounding VIPs		Layers (from Top to Bottom)			
		Assembly Edges	Between VIPS	1	2	3	4
1	3	0.5 in. XPS	1 in. XPS	1 in. XPS	1 in. VIP	1 in.EPS	—
2	3	0.5 in. XPS	1 in. XPS	1 in. EPS	0.5 in. XPS	1 in. VIP	0.5 in. EPS
3	3	0.5 in. XPS	1 in. XPS	1 in. EPS	0.5 in. XPS	1 in. VIP	0.5 in. XPS
4	3	0.04 in. PVC*	0.08 in. PVC*	1 in. EPS	1 in. VIP	1 in. EPS	—
5	1	0.5 in. XPS	1 in. XPS	1 in. EPS	1 in. VIP	1 in. XPS	—
6	3	0.5 in. XPS	1 in. XPS	1 in. XPS	1 in. VIP	1 in. XPS	—
8	3	0.5 in. EPS	1 in. XPS	1 in. EPS	1 in. VIP	1 in. EPS	—
10	2	0.5 in. XPS	Butt joint, edge to edge (not flap to flap)	1 in. XPS	1 in. VIP	1 in. XPS	—

* PVC was approximately 50 mm (2 in.) high, covering the side of the VIP and the side of the bottom foam so that it touched the bottom plate of the apparatus but not the top plate.

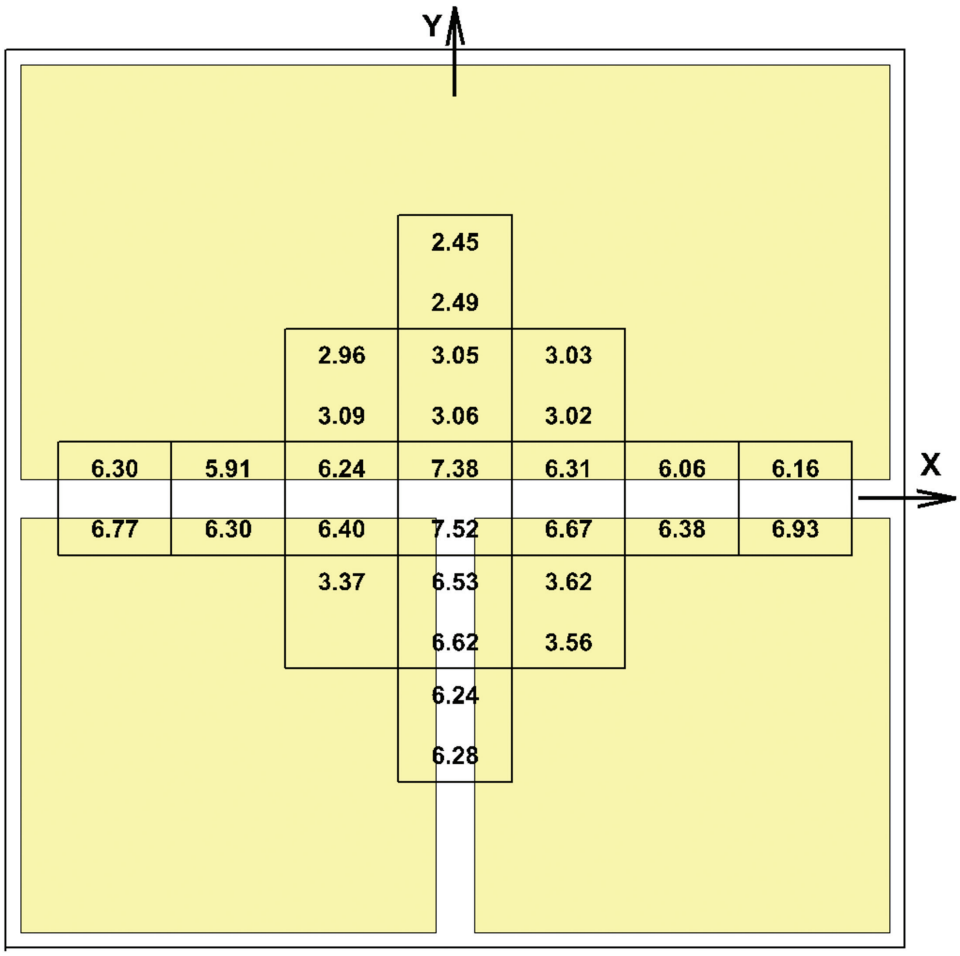

Figure 9 *Fluxes: Design option 1, EPS on bottom, XPS on top.*

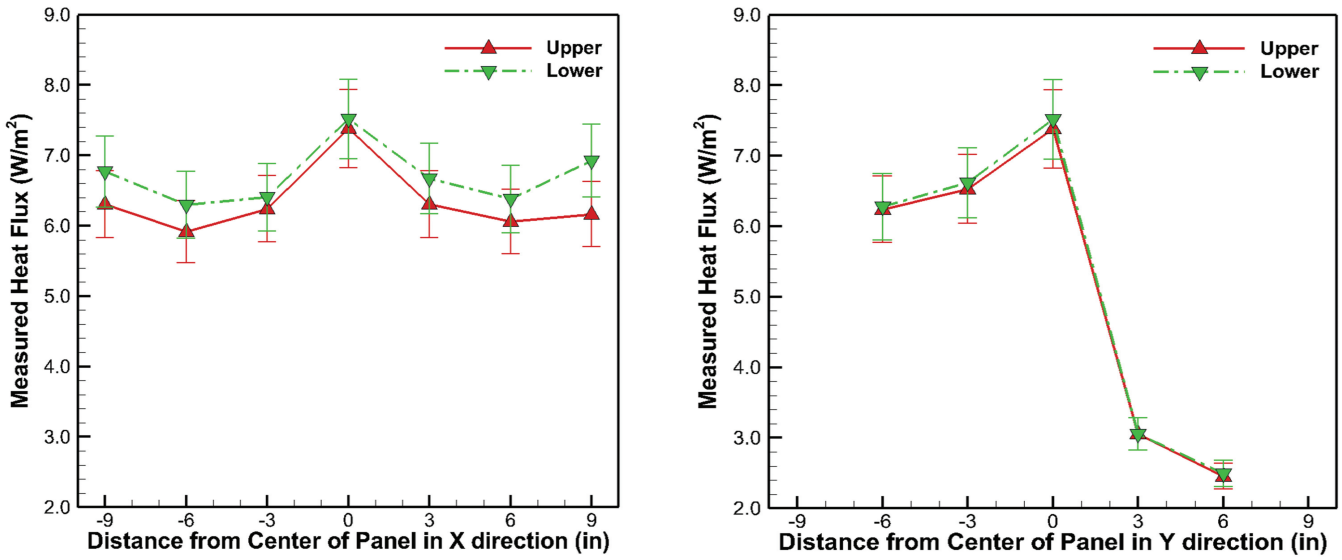

Figure 10 *Upper and lower fluxes along center axes: design option 1.*

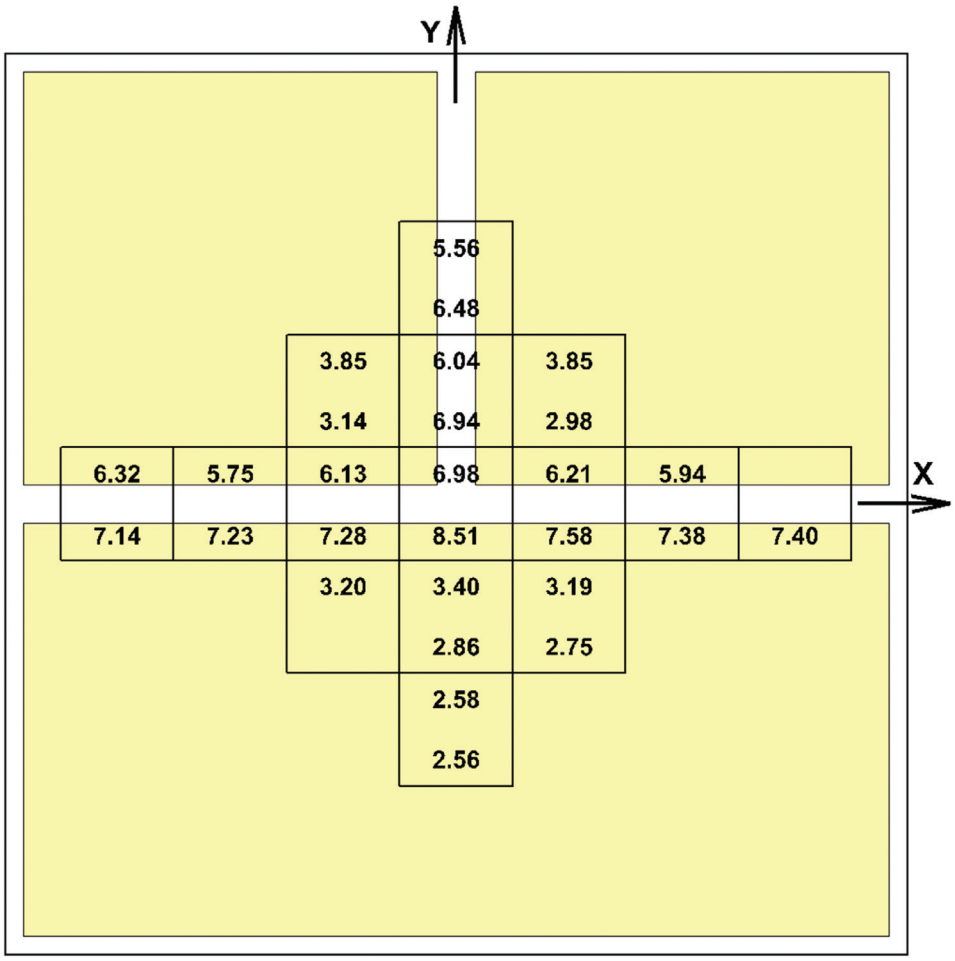

Figure 11 *Design option 2, thin EPS on bottom, EPS and XPS on top.*

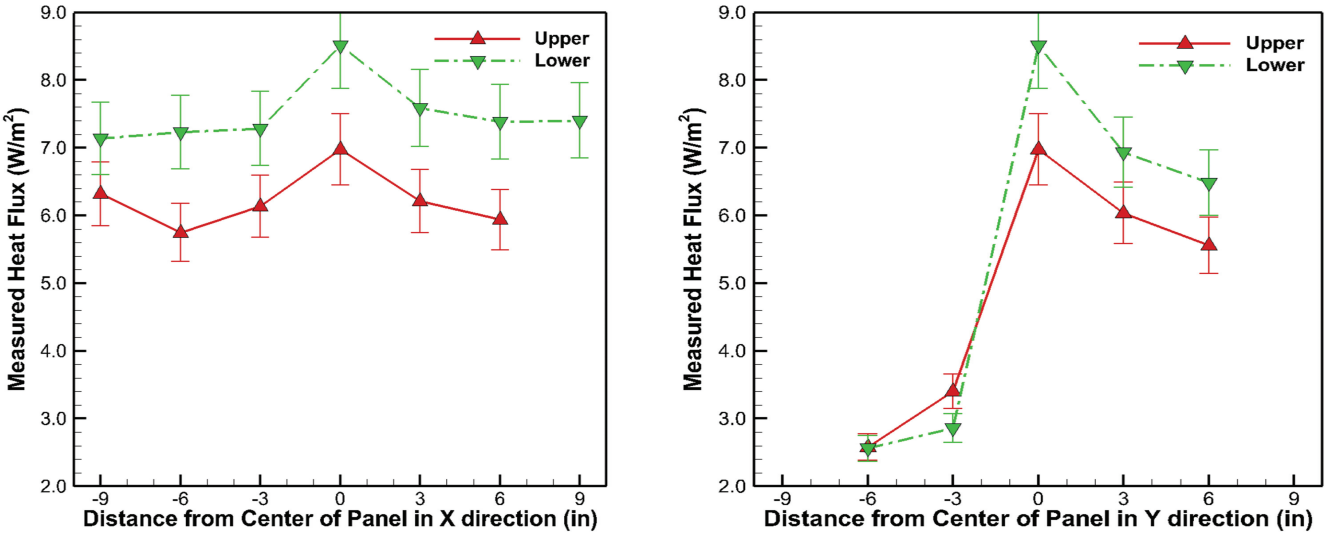

Figure 12 *Upper and lower fluxes along center axes: design option 2.*

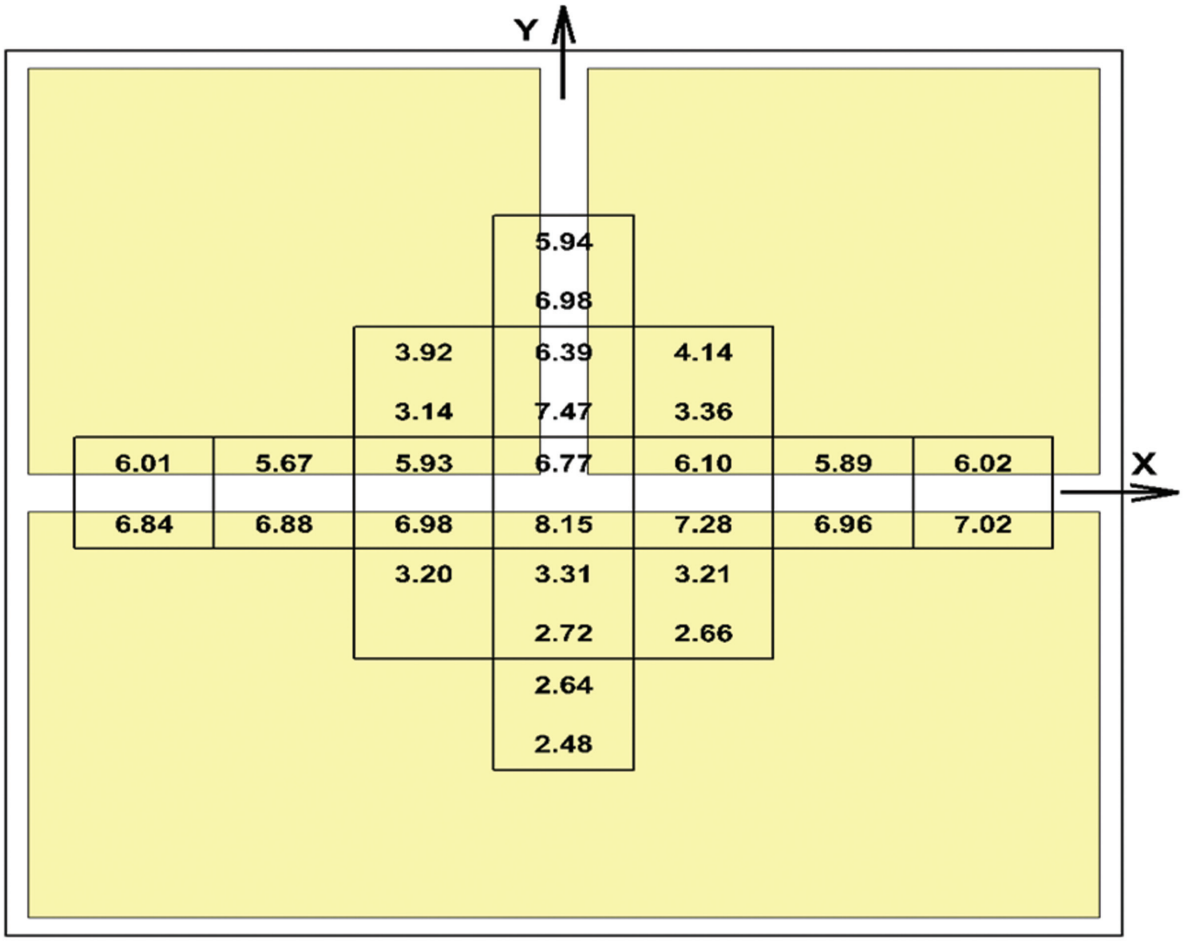

Figure 13 *Fluxes: Design option 3, thin XPS on bottom, EPS and XPS on top.*

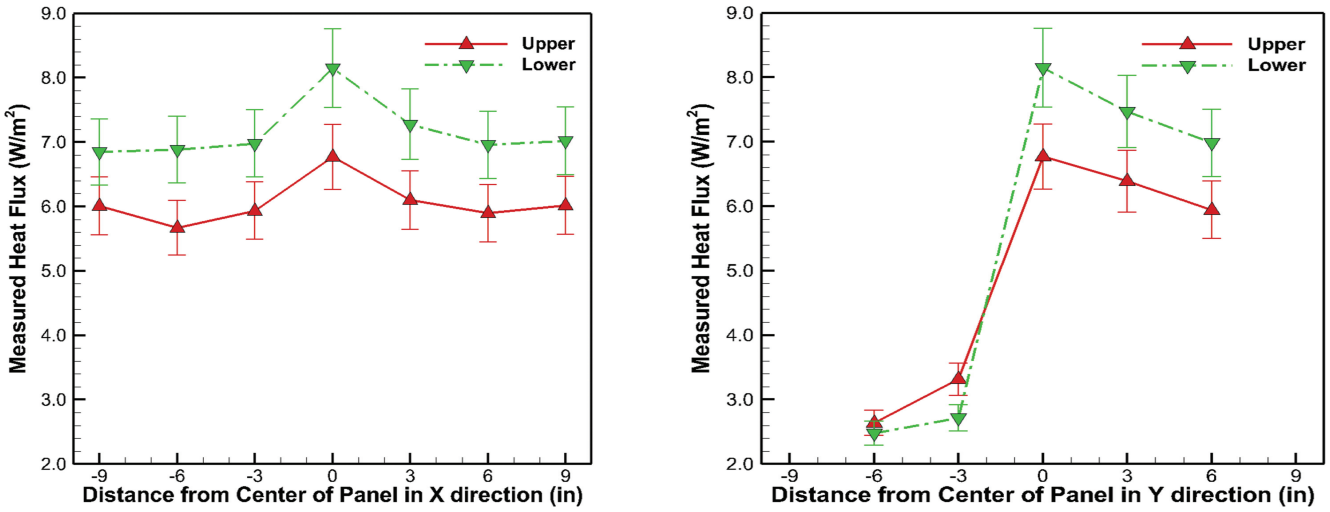

Figure 14 *Upper and lower fluxes along center axes: design option 3.*

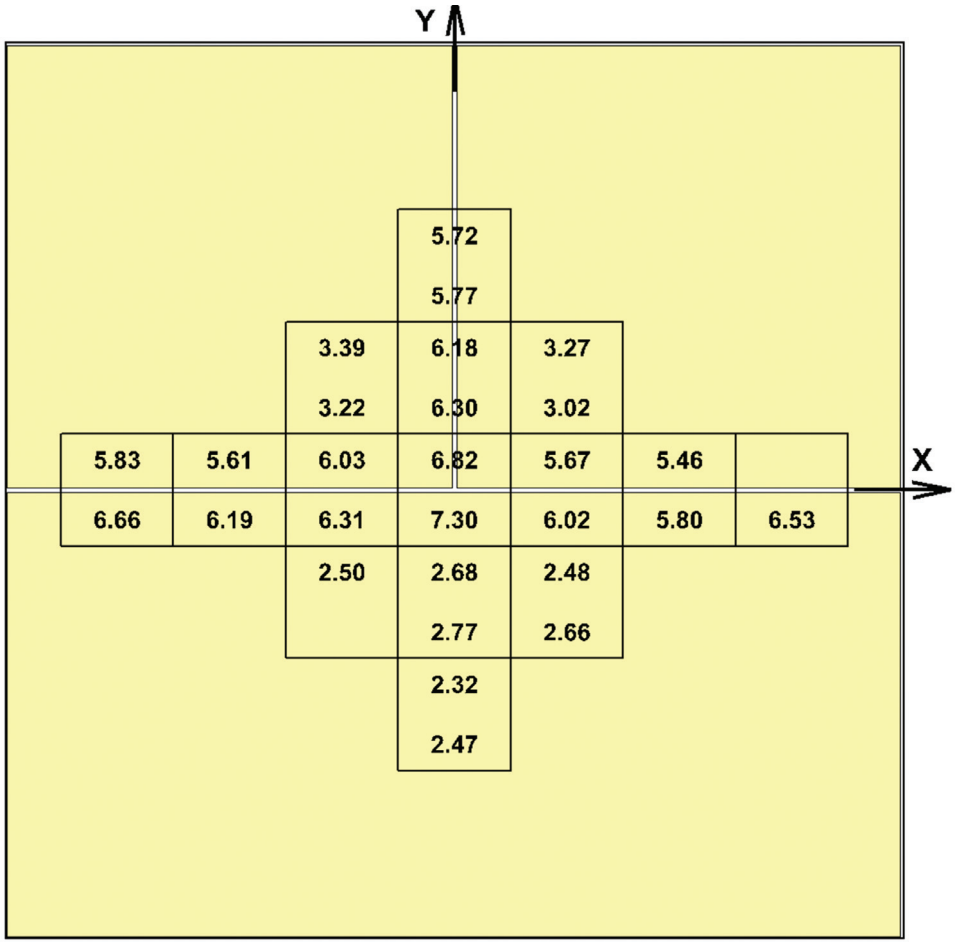

Figure 15 *Fluxes: Design option 4, EPS top and bottom, thin PVC between panels and at edges.*

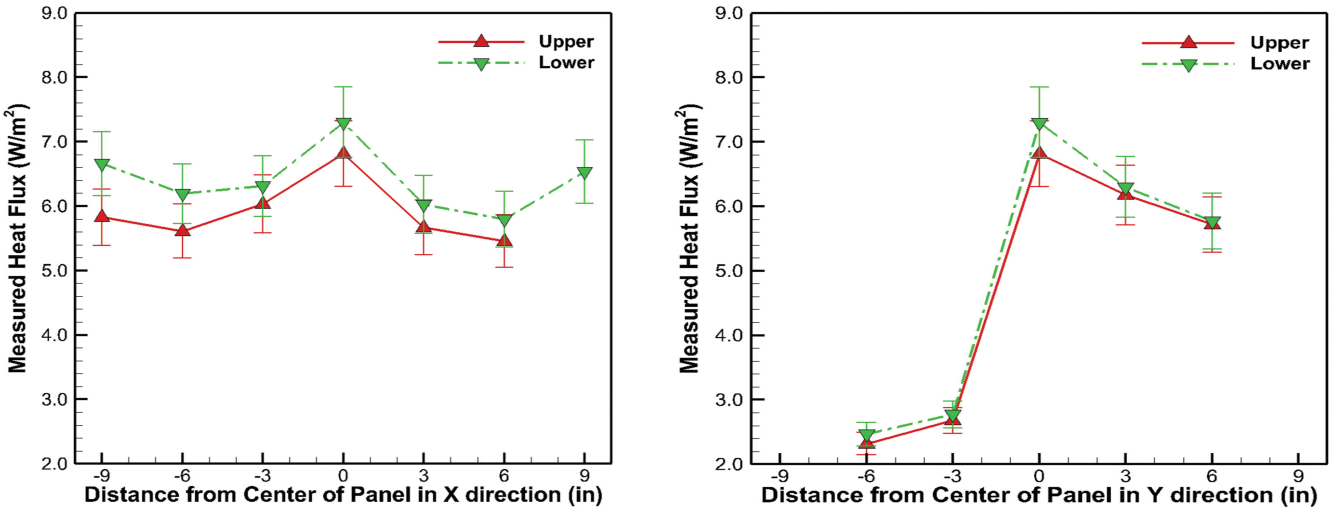

Figure 16 *Upper and lower fluxes along center axes: design option 4.*

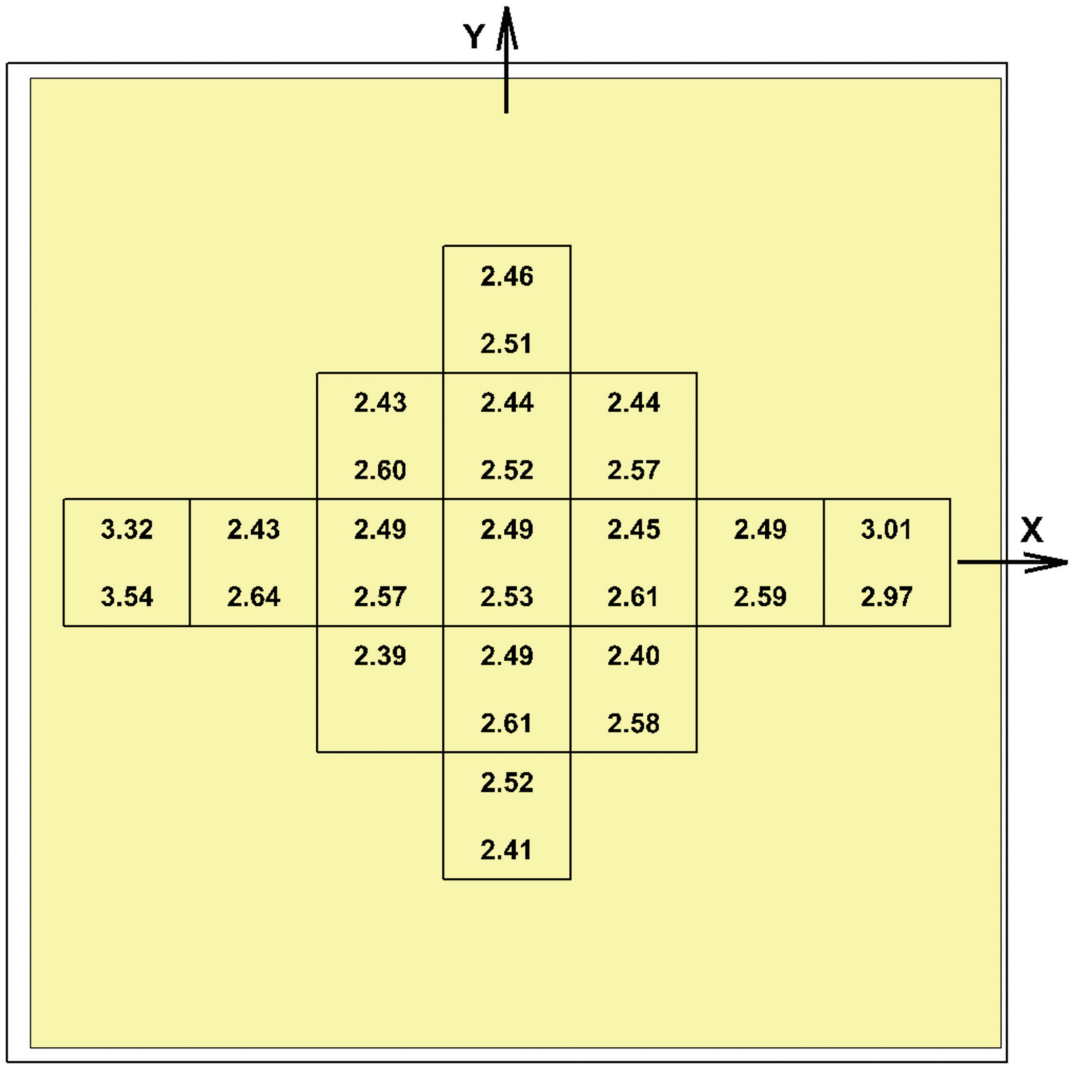

Figure 17 *Design option 5, XPS bottom and EPS top, single large VIP.*

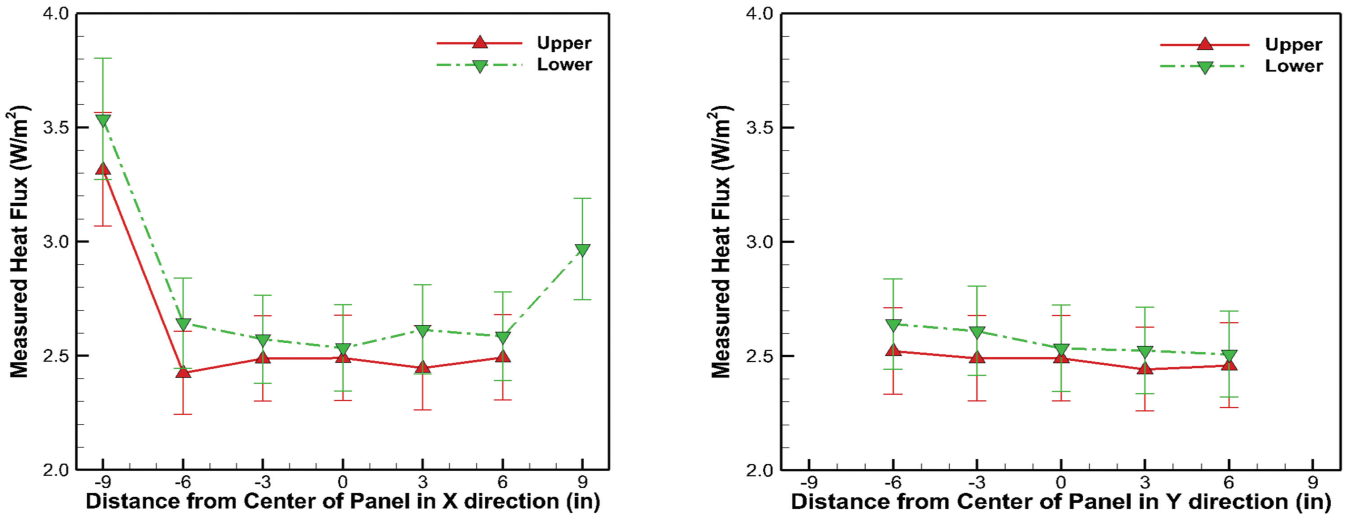

Figure 18 *Upper and lower fluxes along center axes: design option 5.*

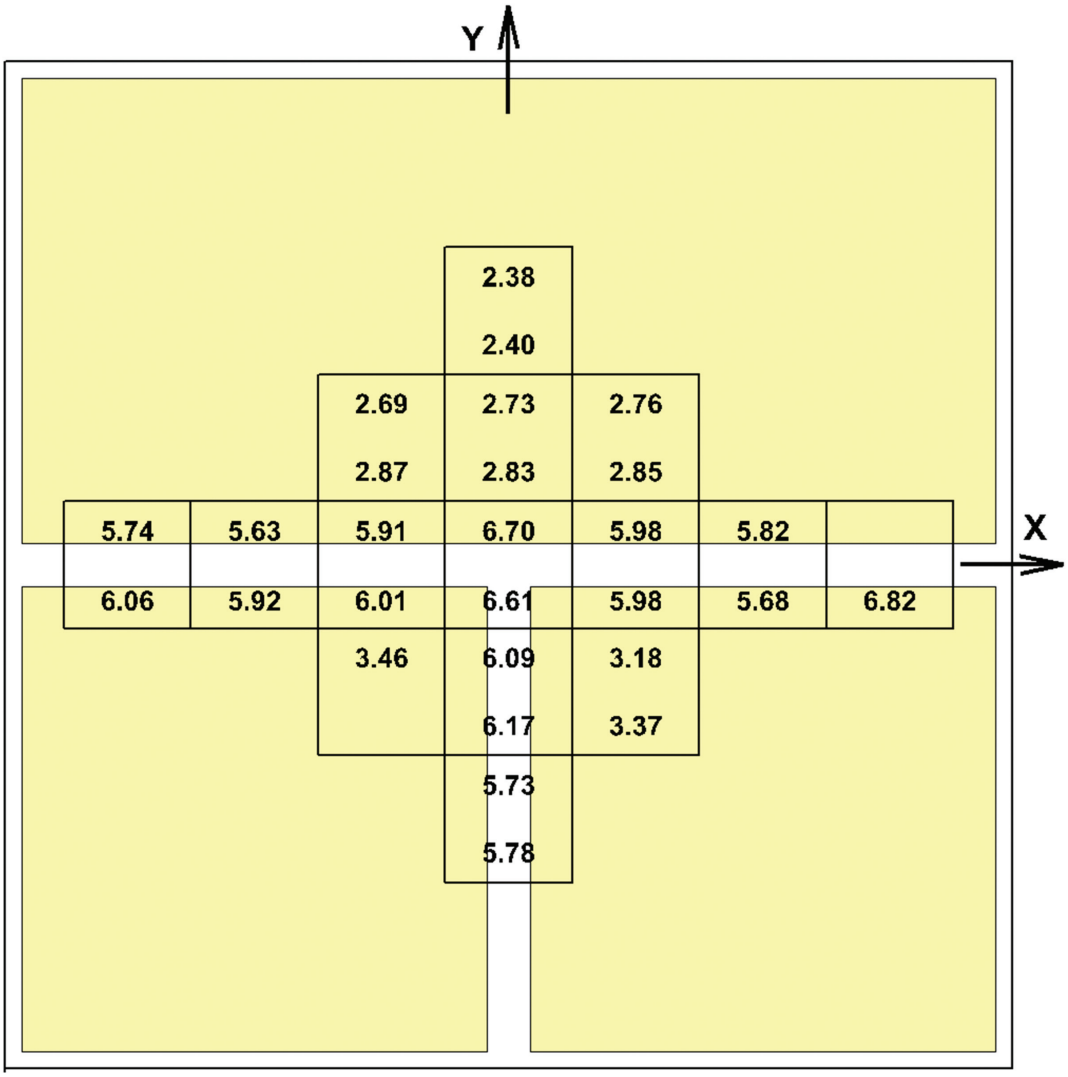

Figure 19 *Fluxes: Design option 6, XPS top and bottom.*

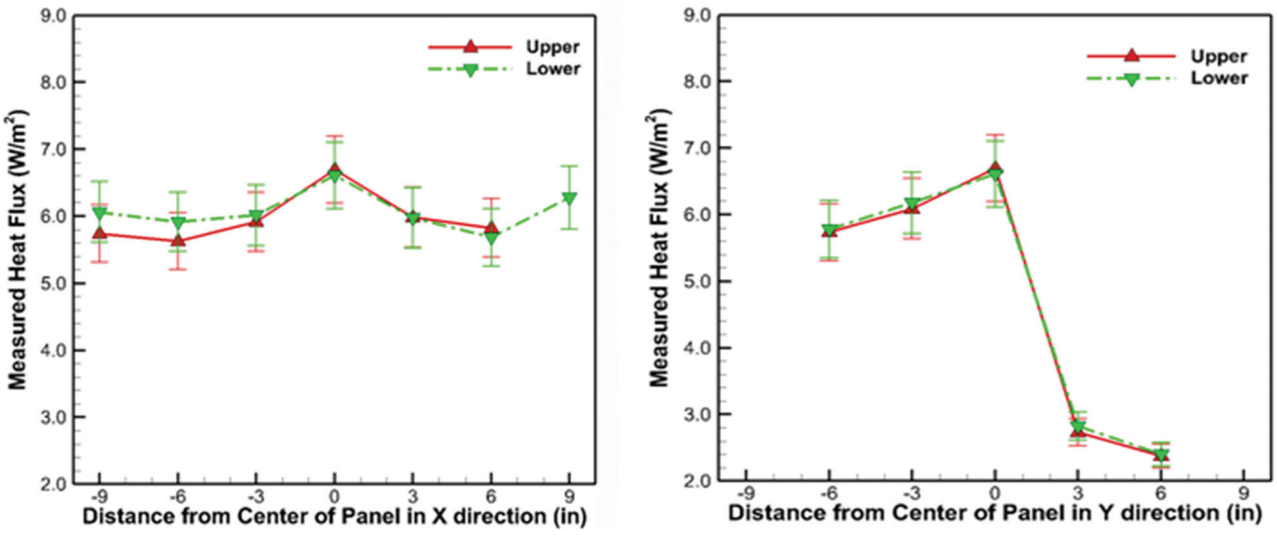

Figure 20 *Upper and lower fluxes along center axes: design option 6.*

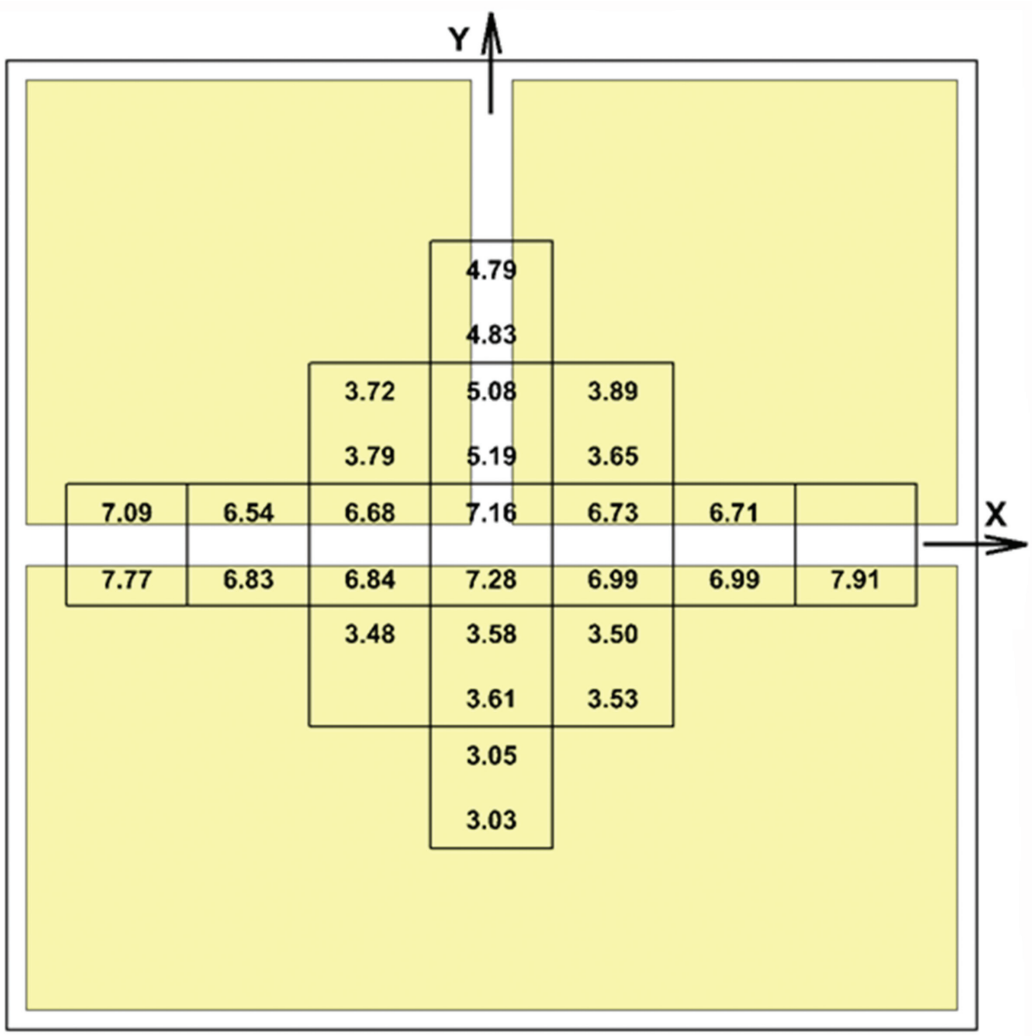

Figure 21 *Fluxes: design option 8, EPS top and bottom.*

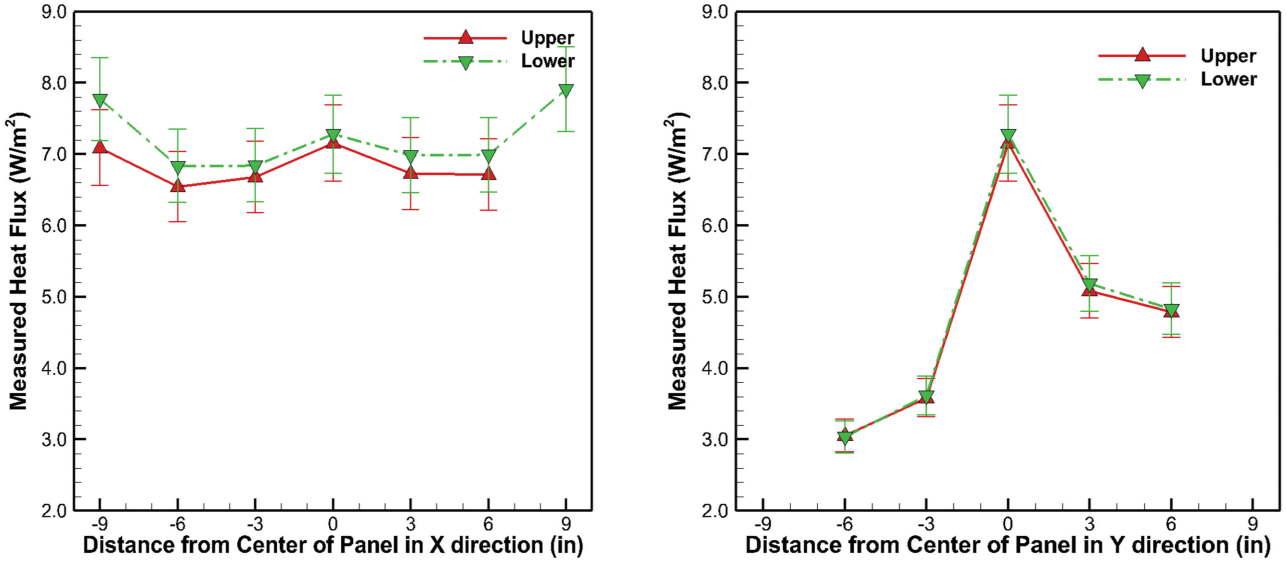

Figure 22 *Upper and lower fluxes along center axes: design option 8.*

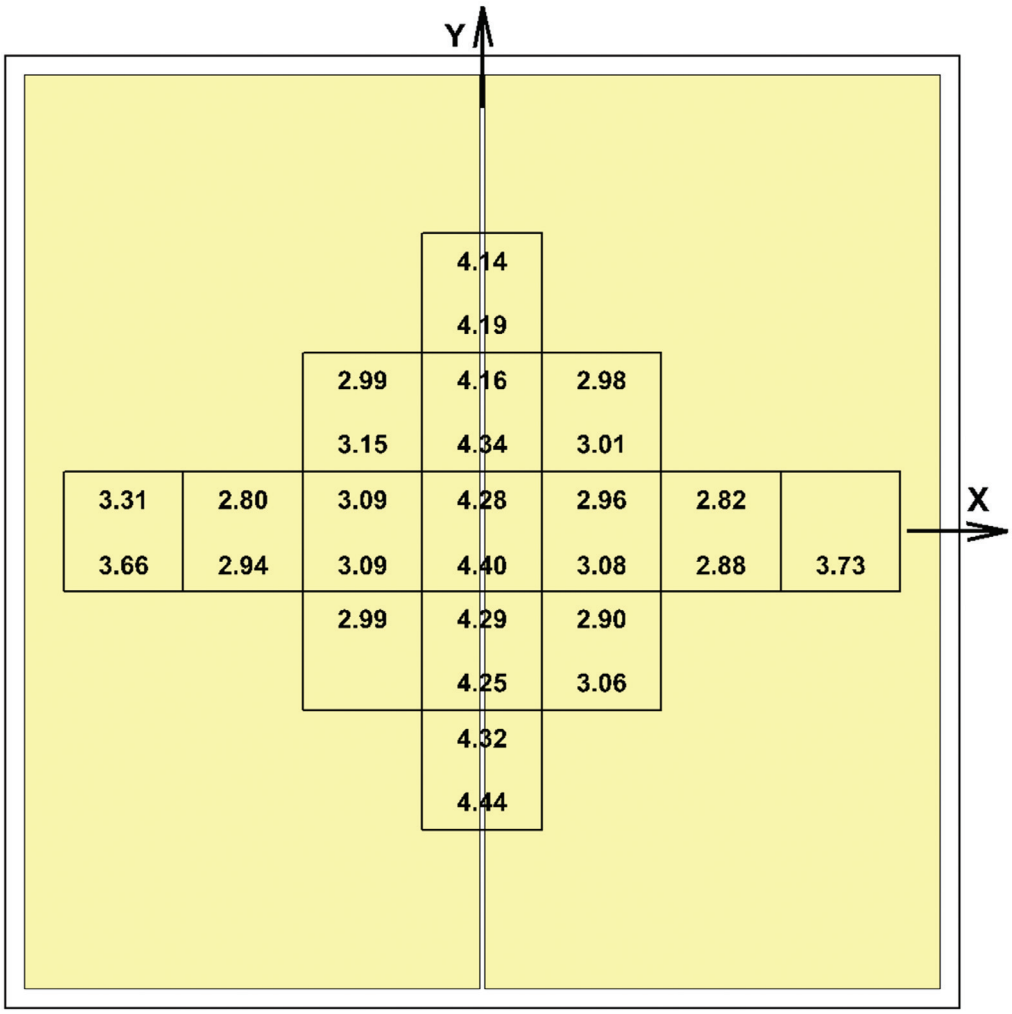

Figure 23 *Design option 10, XPS top and bottom, two half-size VIPs butted together edge to edge in the center.*

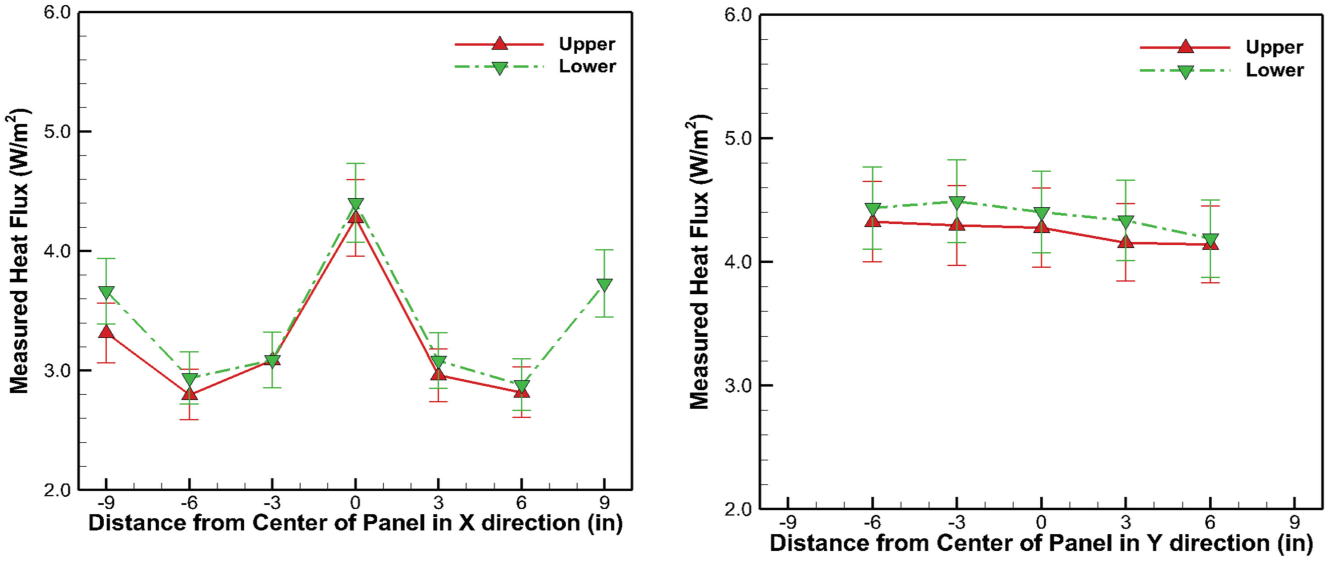

Figure 24 *Upper and lower fluxes along center axes: design option 10.*

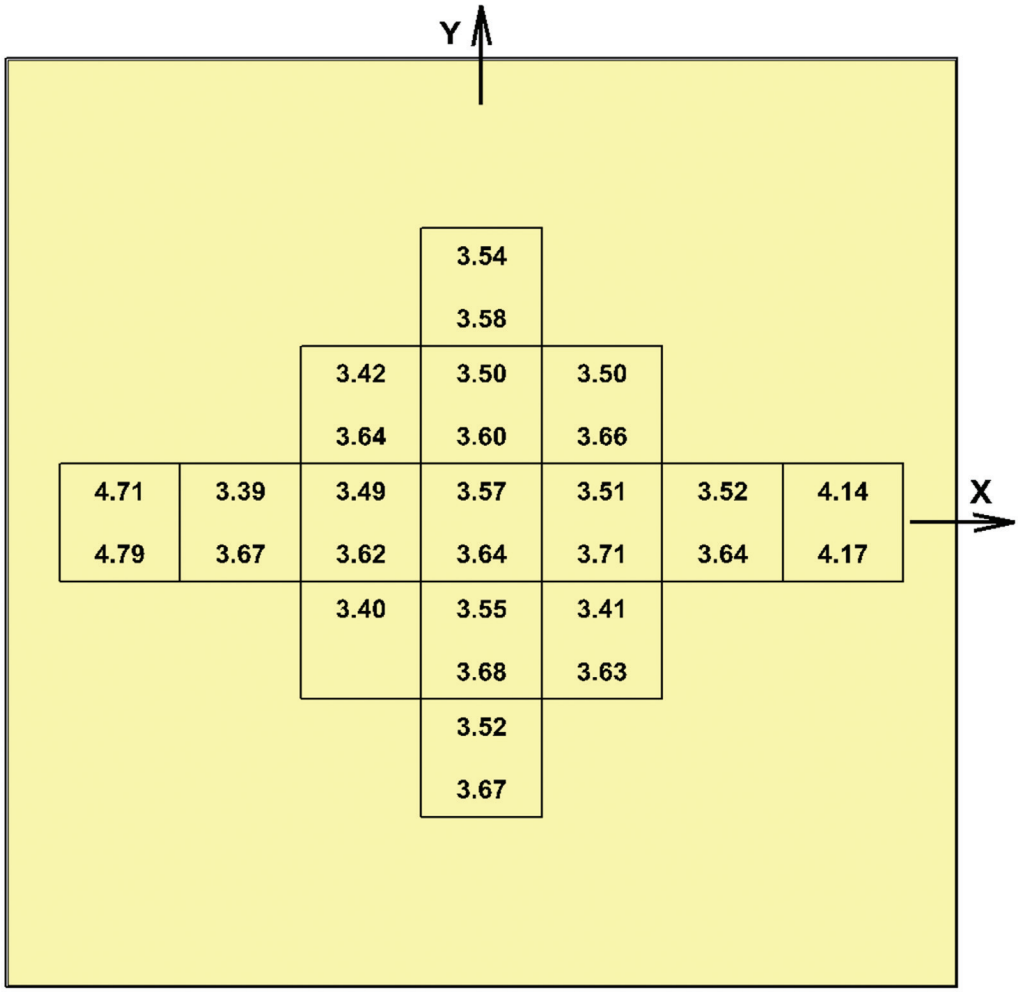

Figure 25 *Fluxes: 23.5 × 23.5 in. VIP #1.*

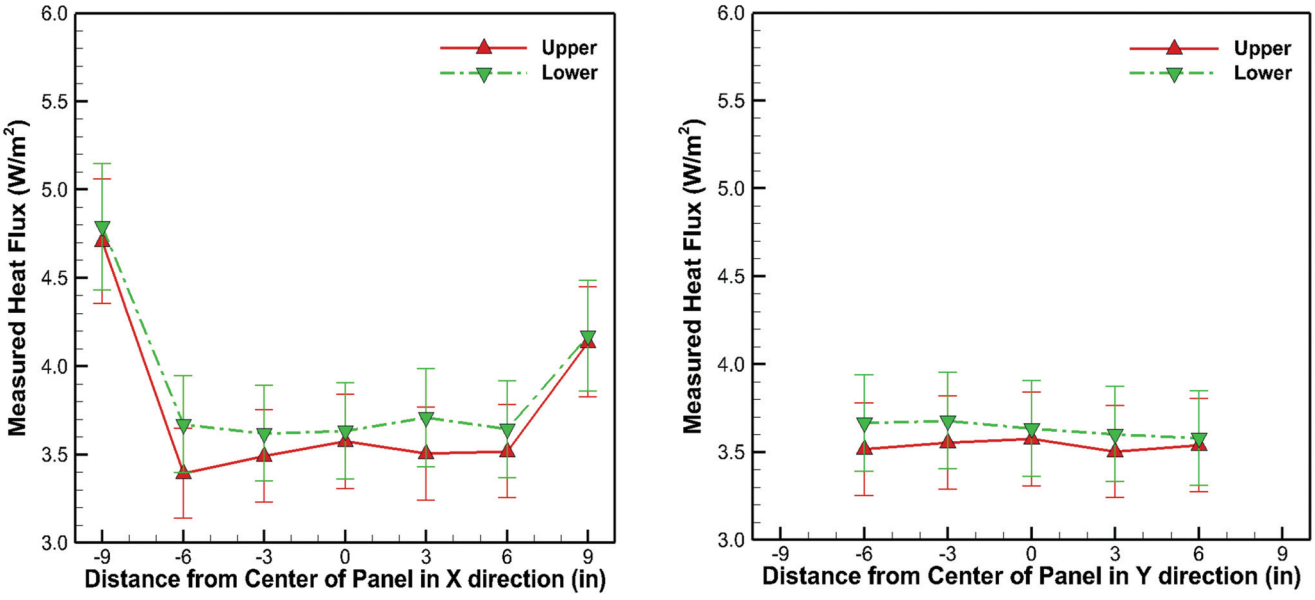

Figure 26 *Upper and lower fluxes along center axes: 23.5 × 23.5 in. VIP #1.*

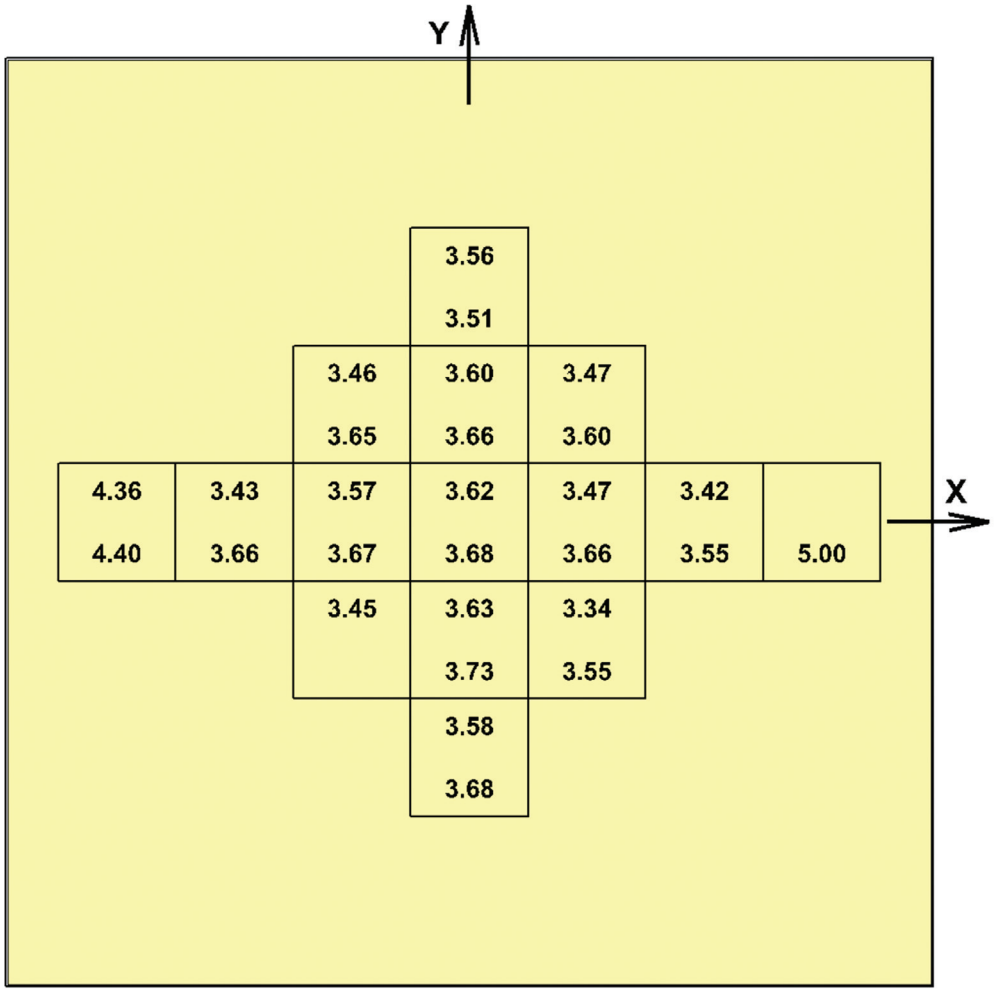

Figure 27 *Fluxes: 23.5 × 23.5 in. VIP #2.*

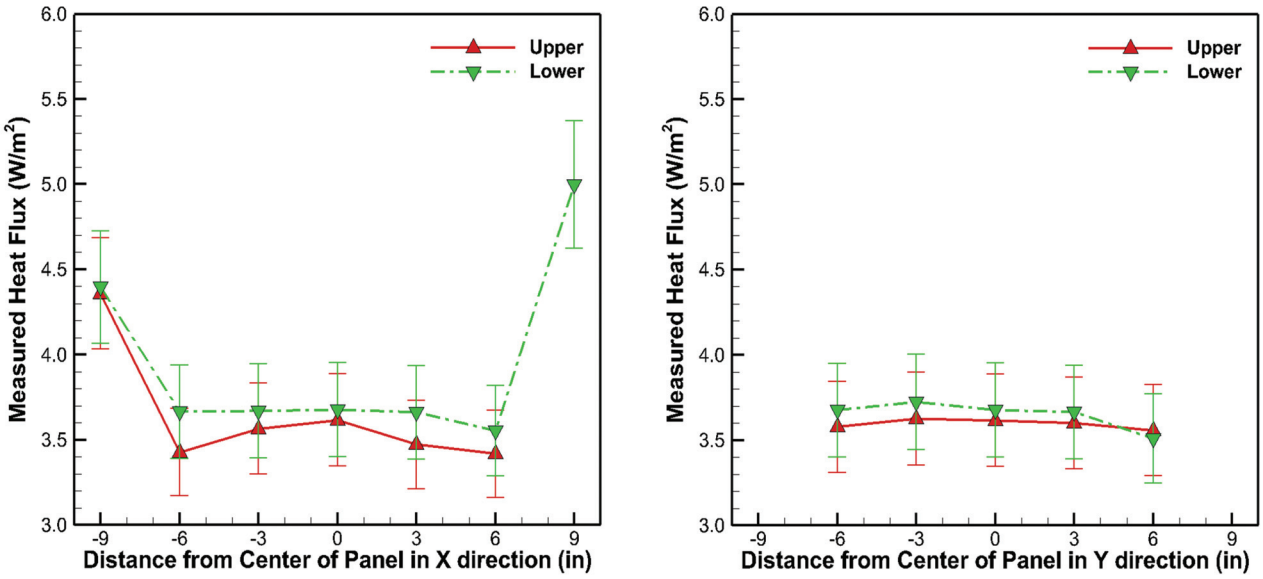

Figure 28 *Upper and lower fluxes along center axes: 23.5 × 23.5 in. VIP #2.*

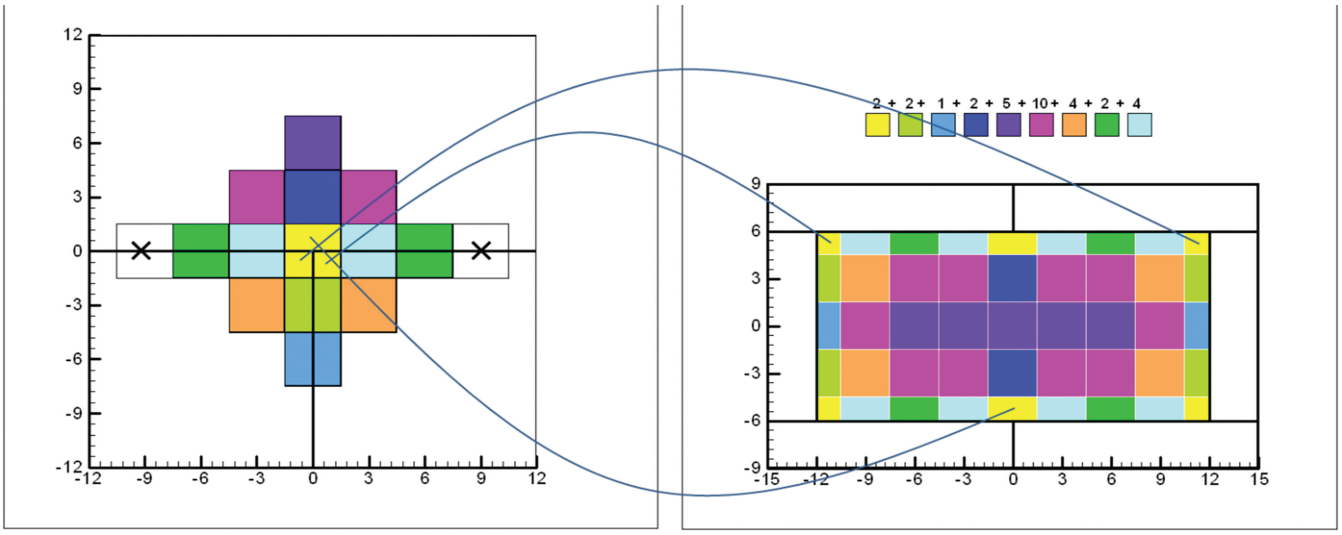

Figure 29 *Mapping HFM data to a staggered array of 12 × 24 in. VIP assemblies.*

heat flux occurs at the center of the specimen, where *x* and *y* are both equal to zero. This is the transducer location with the maximum area of foam insulation and the minimum amount of VIP coverage. As you travel along the *y*-axis in the right half of Figure 10, notice the heat flux drops significantly as the *y*-value increases, which corresponds to the positive *y*-values, or the top half of Figure 9, where the transducer is located over the center of a VIP and farther away from the foam insulation sections.

Design option 1 is symmetric in the *z*-direction (i.e., the thickness of the insulation on the top and the bottom of the VIP are the same), and the top and bottom heat fluxes are very close. Design option 2 on the other hand has only 12.7 mm (0.5 in.) of insulation on the bottom of the VIP and 38.1 mm (1.5 in.) of insulation on the top. Comparing Figure 12 to Figure 10, the difference between the top and bottom plate heat fluxes is much greater for option 2. In option 2, the heat flux along the foam insulation seams is greater on the lower plate, but the heat flux near the center of the panels is less. This can be seen on the *y*-axis profile in Figure 12 and in the numbers displayed for the VIP areas (in yellow) in Figure 11. Notice that the difference between the minimum and maximum flux is less on the upper side where the insulation thickness is greater.

This more uniform heat flux would produce a more uniform temperature distribution on the outside of the thicker foam surface. This may prove useful if there is any concern with regard to ghosting phenomena.[1] However, panels constructed in this manner would have to be clearly marked to ensure proper installation during the construction process.

[1] Ghosting may occur when some portions of a wall are cooler than others, leading to uneven patterns of condensation, which can then lead to uneven patterns of dust accumulation. This occurred on the inside of metal-framed walls in some buildings before exterior insulation became more common for this framing system.

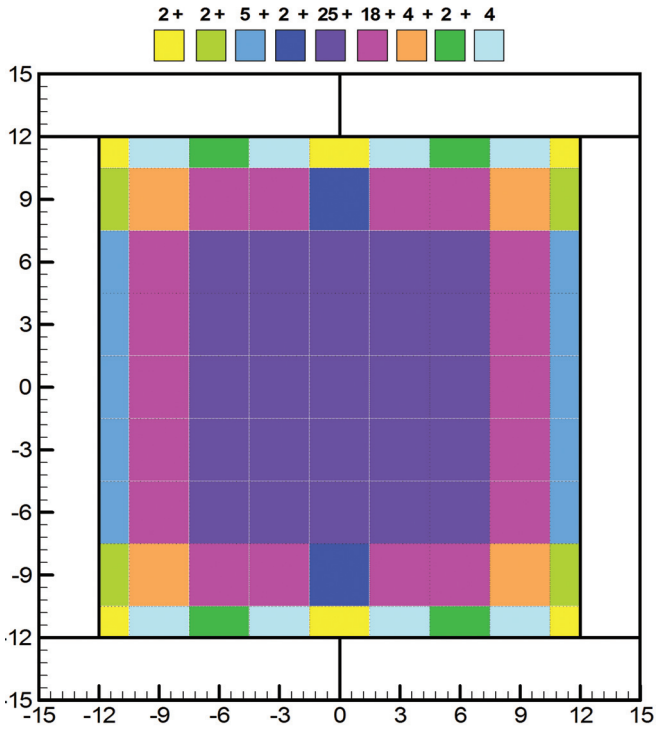

Figure 30 *Mapping HFM data to staggered array of 24 × 24 in. VIP assemblies.*

MAPPING HFT READINGS TO FULL VIP ASSEMBLIES

The test specimens were designed to place the junctions between VIPs directly within the metered areas, and specifically, to center the junctions along a centerline of the transducers. Each transducer reports the average heat flux over a 75 × 75 mm (3 × 3 in.) area. The collection of test specimens

has therefore produced information typical of heat transfer through the center of a panel (purple in the left half of Figure 33), near the corner of a panel (tan), along a straight junction of panels (blues and greens), and at a junction where two corners come together beside the continuous edge of a third panel (yellow). There is no information for a four-corner junction, but such an arrangement is not anticipated in a wall where the units would be staggered to reduce edge losses.

The data from these tests is therefore sufficient to estimate the effective R-value of a VIP-foam panel applied in a staggered array of panels to form a wall. Figures 33 and 34 demonstrate how the HFM readings can be mapped to a 30 × 60 cm

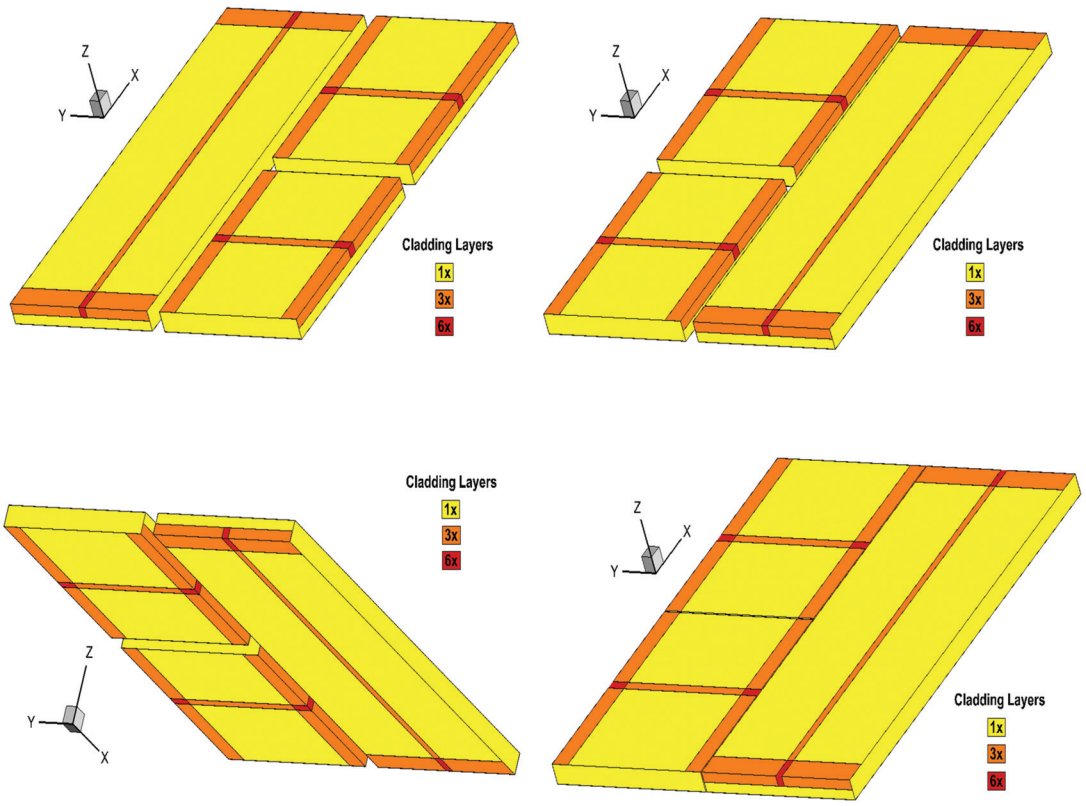

Figure 31 *Number of layers of cladding due to overlap where edges are sealed and wrapping of barrier material around panel: design option 1 (top left), 2 (top right), 3 (bottom left), 4 (bottom right).*

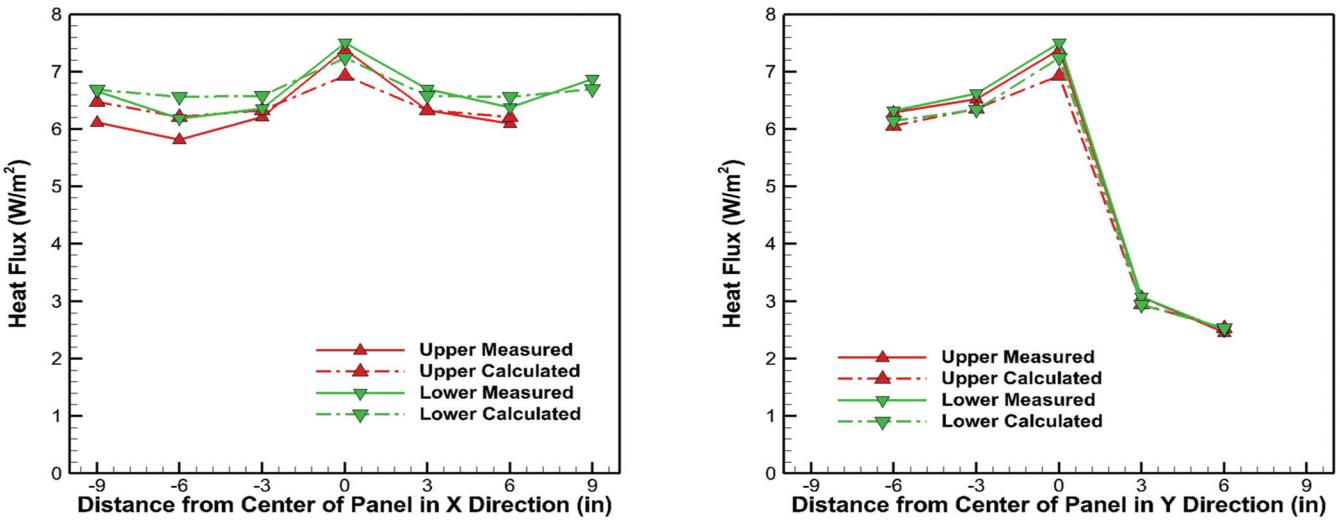

Figure 32 *Measured and calculated fluxes: design option 1.*

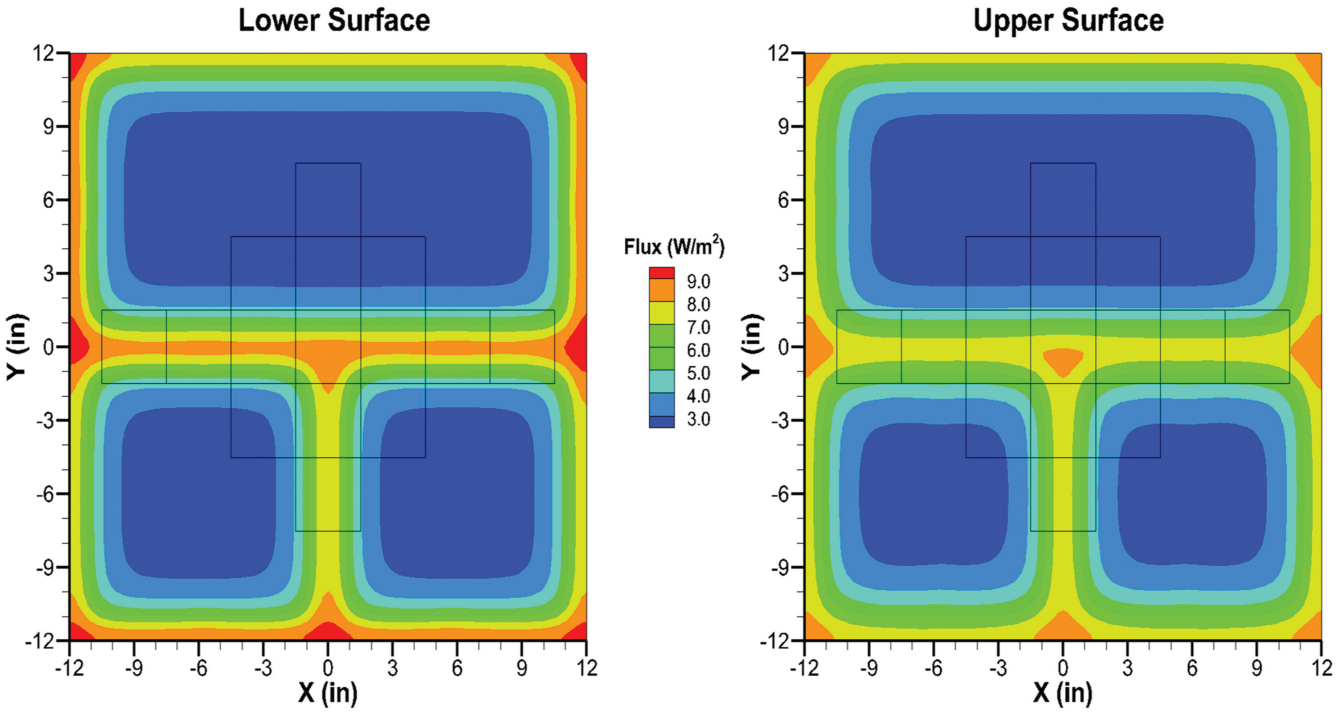

Figure 33 *Calculated flux distributions on lower and upper surfaces: design option 1.*

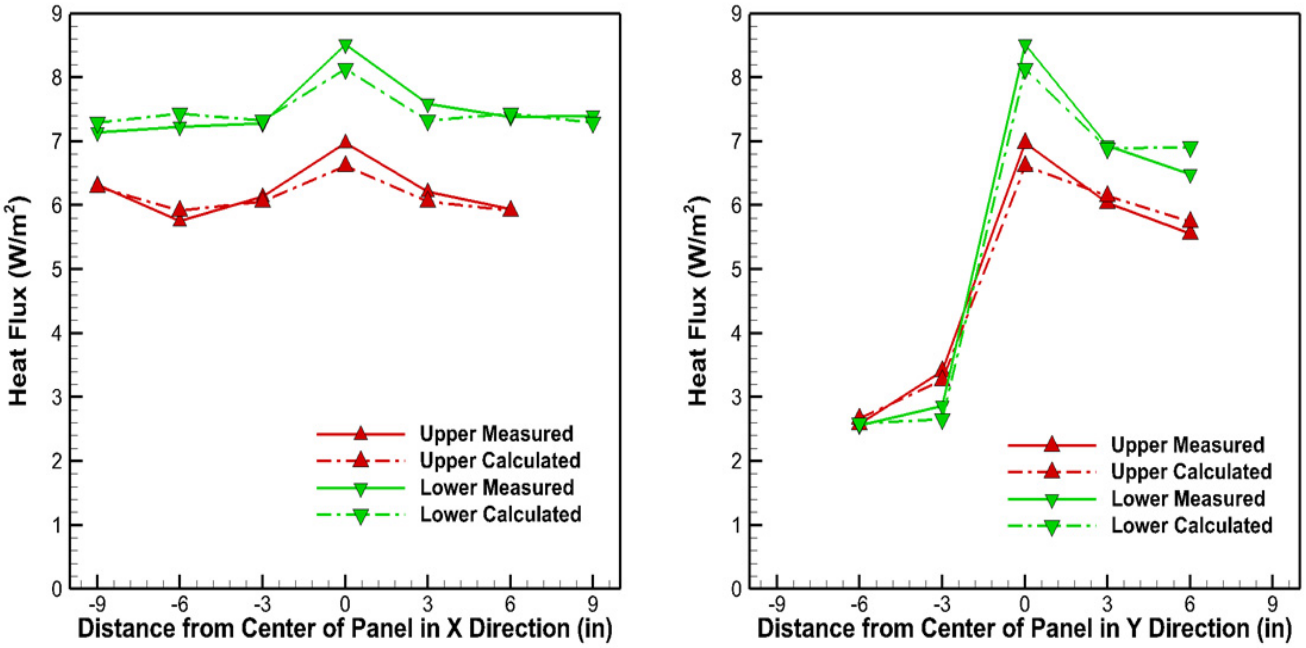

Figure 34 *Measured and calculated fluxes: design option 2.*

Table 2. Mapped Thermal Resistance for Design Option 1 (Test 9716*)

Transducer Color Code	Transducer(s)	Average Flux (W/m^2)	12 × 24 in. Panel Assembly		24 × 24 in. Panel Assembly	
			Area Factor	Product	Area Factor	Product
Yellow	8	7.25	2	14.50	2	14.50
Light green	13	6.37	2	12.74	2	12.74
Medium blue	15	6.11	1	6.11	5	30.56
Dark blue	3	3.06	2	6.11	2	6.11
Purple	1	2.41	5	12.05	25	60.26
Magenta	2, 4	3.00	10	30.04	18	54.07
Orange	12, 14	3.38	4	13.52	4	13.52
Medium green	6, 10	5.99	2	11.97	2	11.97
Light blue	7, 9	6.26	4	25.04	4	25.04
		Area-Weighted Average Flux (W/m^2)		4.13		3.57
		Assembly R-value ($m^2 \cdot K/W$)		5.38		6.22
		Assembly R-value ($h \cdot ft^2 \cdot °F/Btu$)		30.6		35.3

*Test 9716 was determined to have run for an insufficient time; it is only used here as an example of the influence of experimental differences upon the mapping results.

Table 3. Mapped Thermal Resistance for Design Option 1 (Test 9938)

Transducer Color Code	Transducer(s)	Average Flux (W/m^2)	12 × 24 in. Panel Assembly		24 × 24 in. Panel Assembly	
			Area Factor	Product	Area Factor	Product
Yellow	8	7.35	2	14.70	2	14.70
Light green	13	6.74	2	13.47	2	13.47
Medium blue	15	6.40	1	6.40	5	31.98
Dark blue	3	2.92	2	5.83	2	5.83
Purple	1	2.52	5	12.60	25	62.99
Magenta	2, 4	2.81	10	28.12	18	50.62
Orange	12, 14	3.61	4	14.45	4	14.45
Medium green	6, 10	6.29	2	12.59	2	12.59
Light blue	7, 9	6.53	4	26.11	4	26.11
		Area-Weighted Average Flux (W/m^2)		4.20		3.64
		Assembly R-value ($m^2 \cdot K/W$)		5.30		6.11
		Assembly R-value ($h \cdot ft^2 \cdot °F/Btu$)		30.1		34.7

Table 4. Mapped Thermal Resistance for Design Option 2 (Test 9953)

Transducer Color Code	Transducer(s)	Average Flux (W/m^2)	12 × 24 in. Panel Assembly		24 × 24 in. Panel Assembly	
			Area Factor	Product	Area Factor	Product
Yellow	8	7.75	2	15.49	2	15.49
Light green	3	6.49	2	12.97	2	12.97
Medium blue	1	6.02	1	6.02	5	30.10
Dark blue	13	3.13	2	6.26	2	6.26
Purple	15	2.57	5	12.85	25	64.26
Magenta	12, 14	2.97	10	29.74	18	53.53
Orange	2, 4	3.46	4	13.83	4	13.83
Medium green	6, 10	6.57	2	13.15	2	13.15
Light blue	7, 9	6.80	4	27.21	4	27.21
		Area-Weighted Average Flux (W/m^2)		4.30		3.70
		Assembly R-value ($m^2 \cdot K/W$)		5.17		6.01
		Assembly R-value ($h \cdot ft^2 \cdot °F/Btu$)		29.4		34.1

Table 5. Mapped Thermal Resistance for Design Option 3 (Test 9954)

Transducer Color Code	Transducer(s)	Average Flux (W/m^2)	12 × 24 in. Panel Assembly		24 × 24 in. Panel Assembly	
			Area Factor	Product	Area Factor	Product
Yellow	8	7.46	2	14.92	2	14.92
Light green	3	6.93	2	13.86	2	13.86
Medium blue	1	6.46	1	6.46	5	32.31
Dark blue	13	3.01	2	6.03	2	6.03
Purple	15	2.56	5	12.79	25	63.95
Magenta	12, 14	2.93	10	29.30	18	52.74
Orange	2, 4	3.64	4	14.57	4	14.57
Medium green	6, 10	6.35	2	12.70	2	12.70
Light blue	7, 9	6.57	4	26.29	4	26.29
		Area-Weighted Average Flux (W/m^2)		4.28		3.71
		Assembly R-value ($m^2 \cdot K/W$)		5.19		5.99
		Assembly R-value ($h \cdot ft^2 \cdot °F/Btu$)		29.5		34.0

Table 6. Mapped Thermal Resistance for Design Option 4 (Test 9763)

Transducer Color Code	Transducer(s)	Average Flux (W/m^2)	12 × 24 in. Panel Assembly		24 × 24 in. Panel Assembly	
			Area Factor	Product	Area Factor	Product
Yellow	8	7.06	2	14.12	2	14.12
Light green	3	6.24	2	12.47	2	12.47
Medium blue	1	5.74	1	5.74	5	28.72
Dark blue	13	2.72	2	5.45	2	5.45
Purple	15	2.39	5	11.95	25	59.77
Magenta	12, 14	2.57	10	25.73	18	46.32
Orange	2, 4	3.23	4	12.91	4	12.91
Medium green	6, 10	5.76	2	11.53	2	11.53
Light blue	7, 9	6.01	4	24.03	4	24.03
Area-Weighted Average Flux (W/m^2)				3.87		3.36
Assembly R-value ($m^2 \cdot K/W$)				5.74		6.60
Assembly R-value ($h \cdot ft^2 \cdot °F/Btu$)				32.6		37.5

Table 7. Mapped Thermal Resistance for Design Option 6 (Test 9955)

Transducer Color Code	Transducer(s)	Average Flux (W/m^2)	12 × 24 in. Panel Assembly		24 × 24 in. Panel Assembly	
			Area Factor	Product	Area Factor	Product
Yellow	8	6.65	2	13.30	2	13.30
Light green	13	6.13	2	12.26	2	12.26
Medium blue	15	5.75	1	5.75	5	28.77
Dark blue	3	2.78	2	5.56	2	5.56
Purple	1	2.39	5	11.94	25	59.69
Magenta	2, 4	2.80	10	27.95	18	50.32
Orange	12, 14	3.35	4	13.39	4	13.39
Medium green	6, 10	5.76	2	11.52	2	11.52
Light blue	7, 9	5.97	4	23.88	4	23.88
Area-Weighted Average Flux (W/m^2)				3.92		3.42
Assembly R-value ($m^2 \cdot K/W$)				5.66		6.50
Assembly R-value ($h \cdot ft^2 \cdot °F/Btu$)				32.2		36.9

Table 8. Mapped Thermal Resistance for Design Option 8 (Test 9956)

Transducer Color Code	Transducer(s)	Average Flux (W/m^2)	12 × 24 in. Panel Assembly		24 × 24 in. Panel Assembly	
			Area Factor	Product	Area Factor	Product
Yellow	8	7.22	2	14.43	2	14.43
Light green	3	5.13	2	10.27	2	10.27
Medium blue	1	4.81	1	4.81	5	24.04
Dark blue	13	3.60	2	7.20	2	7.20
Purple	15	3.04	5	15.21	25	76.07
Magenta	12, 14	3.51	10	35.07	18	63.12
Orange	2, 4	3.76	4	15.05	4	15.05
Medium green	6, 10	6.77	2	13.54	2	13.54
Light blue	7, 9	6.81	4	27.24	4	27.24
Area-Weighted Average Flux (W/m^2)				4.46		3.92
Assembly R-value ($m^2 \cdot K/W$)				4.98		5.67
Assembly R-value ($h \cdot ft^2 \cdot °F/Btu$)				28.3		32.2

Table 9. Summary and Ranking of Mapped Thermal Resistance

Ranking (Best to Worst)	Design Option	Assembly R-value	
		12 × 24 in. Panel	24 × 24 in. Panel
1	4	32.6	37.5
2	6	32.2	36.9
3	1	29.9	34.5
4/5	2	29.4	34.1
	3	29.5	34.0
6	8	28.3	32.2

(12 × 24 in.) or a 60 × 60 cm (24 × 24 in.) panel. For this technique to work, the gaps between VIPs have to be centered over the HFTs, as was done here. Also there is an inherent assumption that the edge effects are not significant for a transducer that is centered 15 cm (6 in.) from the edge of a VIP.

The following tables give estimates of the effective R-value for design options 1, 2, 3, 4, 6, 8, 11, and 12. The heat flux listed is the average of the top and bottom fluxes for the transducer locations listed. Option 1 was tested multiple times. Two sets of these results are given for design option 1 to get an indication of how much the variability in measurements affects the estimated R-value. The two cases that are compared are the ones with the lowest measured fluxes (9716) and the highest measured fluxes (9938). There is a difference in estimated R-value from the two tests of about 2.1% for a 30 × 60 cm (12 × 24 in.) panel and about 1.8% for a 60 × 60 cm (24 × 24 in.) panel.

The design options are ranked from best to worst based on effective R-value in Table 11.

EXTRACTION OF VIP THERMALPROPERTIES FROM TEST DATA

While mapping HFT values, as presented in the previous section, can be useful in determining the performance of specific design options that have been tested, it does not allow the exploration of alternate design options that have not been tested. Numerical modeling is an option for the exploration of alternate designs that have not been tested, but this is only possible if thermal properties of the VIPs are known. The key VIP properties needed for the numerical model are: (1) the effective core thermal conductivity, which influences the amount of heat conducted through the VIP and (2) the product of the barrier material's thickness and thermal conductivity, which influences the amount of heat conducted around the edges of the VIP. This section presents a methodology for extracting these properties utilizing the data collected from HFM experiments.

The main purpose of running a test with a single large VIP is to obtain a center-of-panel effective core thermal conductivity. Design option 5 contains a single large VIP. The measured heat flux and temperature difference across the assembly can be used to obtain a center-of-panel R-value for the assembly. Since the thickness and temperature-dependent thermal conductivities of the rigid foam layers are known, their contribution to the total R-value can be removed to give the center-of-panel R-value for the VIP. The VIP center-of-panel R-value is then used to calculate an effective core thermal conductivity for the VIP. The effective core thermal conductivity was determined using the data from four separate tests of design option 5. The conductivity was first calculated using the measured heat flux at the center of the panel (transducer #8). The conductivity was calculated three ways: using the flux measured on the upper plate, using the flux measured on the lower plate, and using the average of the flux on the

Table 10. Effective Core Thermal Conductivity (W/m·K) Derived from Tests of Design Option 5

Test	Center Transducer Only (Transducer 8)			Average of Central Nine Transducers (Transducers 2, 3, 4, 7, 8, 9, 12, 13 ,14)		
	Upper	Lower	Average U and L	Upper	Lower	Average U and L
9767	0.00344	0.00351	0.00348	0.00337	0.00358	0.00348
9907	0.00349	0.00355	0.00352	0.00341	0.00360	0.00350
9909	0.00350	0.00354	0.00352	0.00343	0.00359	0.00351
9913	0.00350	0.00353	0.00351	0.00343	0.00358	0.00350
Average	0.00348	0.00353	0.00351	0.00341	0.00359	0.00350

Table 11. Effective Core Thermal Conductivity (W/m·K) Derived from Tests of 600 × 600 mm (23.5 × 23.5 in.) VIPs

Test	Center Transducer Only (Transducer 8)			Average of Central Nine Transducers (Transducers 2–4, 7–9, 12–14)		
	Upper	Lower	Average U and L	Upper	Lower	Average U and L
9822	0.00427	0.00438	0.00433	0.00417	0.00391	0.00403
9825	0.00432	0.00443	0.00438	0.00420	0.00391	0.00405
Average	0.00430	0.00441	0.00436	0.00419	0.00391	0.00404

upper and lower plate. Using this center transducer, the difference between the thermal conductivities calculated from the upper plate flux and lower plate flux is less than 2% for all tests. When using the average of the central nine transducers, the upper to lower difference is as much as 6%; but this difference is still within the experimental uncertainty the measured heat fluxes. The average of the central nine transducers is probably a better indication of the true flux than a single value at the center, so the best estimate of the core conductivity from these tests is 0.0035 W/m·K.

Two bare VIPs were also tested in the same HFM apparatus. These VIPs are not part of an assembly and are nominally 600 mm (23.5 in.) square. The effective core thermal conductivity calculated from these tests is given in Table 11, and is about 15% greater than that of the VIPs within the composite test specimens. These VIPs were manufactured in May 2011 by the same manufacturer as those used in the test assemblies. The difference between the two sets of VIPs is unknown. Design option 5 was disassembled, and the VIP was tested by itself to see if there was something about the assembly that may have skewed the calculated core conductivity for the panel. The resulting core conductivity from the test of the VIP alone was within 2% of the value obtained from testing of the assembly.

In addition to direct measurements of VIP properties, numerical models can be used to extract this information from the array of heat flux data generated by the HFM apparatus test. Therefore, detailed three-dimensional models of several of the VIP test assemblies were developed using the Oak Ridge National Library-developed (ORNL) heat transfer program HEATING (Childs 1993). All of the assemblies consist of one or more VIPs sandwiched between layers of rigid foam insulation.

These models include details such as the multiple layers of barrier material present on some portions of the VIPs due to the way edges are sealed and wrapped around the panel. It is not known a priori if these details significantly impact the overall performance of the assembly, but they may significantly impact the reading of a transducer placed directly over the edge. Therefore it is important to include them in the model used to extract properties from transducer readings. Unfortunately there are other features of the VIP assemblies that are not included in the model. For example, the amount, distribution, and properties of the silicone adhesive used to adhere the VIP to the foam within the test samples are not known. The size and location of small gaps between components and misalignment of the VIPs are also not known.

The models calculate the average heat flux that would be seen by each of the 30 transducers in the HFM apparatus. The HEATING model is coupled with an optimization procedure that varies the VIP properties (effective core thermal conductivity and the conductivity-thickness product of the barrier) to find the combination that gives the best match between the measured and calculated heat fluxes. The best match is defined as the combination that minimizes the function shown in Equation 3.

$$F = \frac{\sum_{i=1}^{n} W_i \left(q_{i-\text{meas}} - q_{i-\text{calc}}\right)^2}{\sum_{i=1}^{n} W_i} \quad (3)$$

where W_i is a weighting factor. The weighting factors are assigned based on the approximate proportion of the overall area that the area covered by a transducer represents.

Detailed models were developed for the first four design options as shown in Figure 35.

Table 12. Effective Thermal Conductance of Vacuum Insulation Panel Components

Design Option (Test ID)	Use All Available Transducers		Exclude Edge Transducers (5 & 11)	
	Barrier $k \times t$ (W/K)	Effective Core k (W/m·K)	Barrier $k \times t$ (W/K)	Effective Core k (W/m·K)
1 (9936)	2.28×10^{-4}	3.49×10^{-3}	2.31×10^{-4}	3.48×10^{-3}
2 (9953)	1.89×10^{-4}	3.59×10^{-3}	1.89×10^{-4}	3.59×10^{-3}
3 (9954)	2.54×10^{-4}	3.53×10^{-3}	2.74×10^{-4}	3.51×10^{-3}
4 (9763)	1.25×10^{-4}	3.25×10^{-3}	1.18×10^{-4}	3.25×10^{-3}
Average of 1–3	2.24×10^{-4}	3.54×10^{-3}	2.31×10^{-4}	3.53×10^{-3}

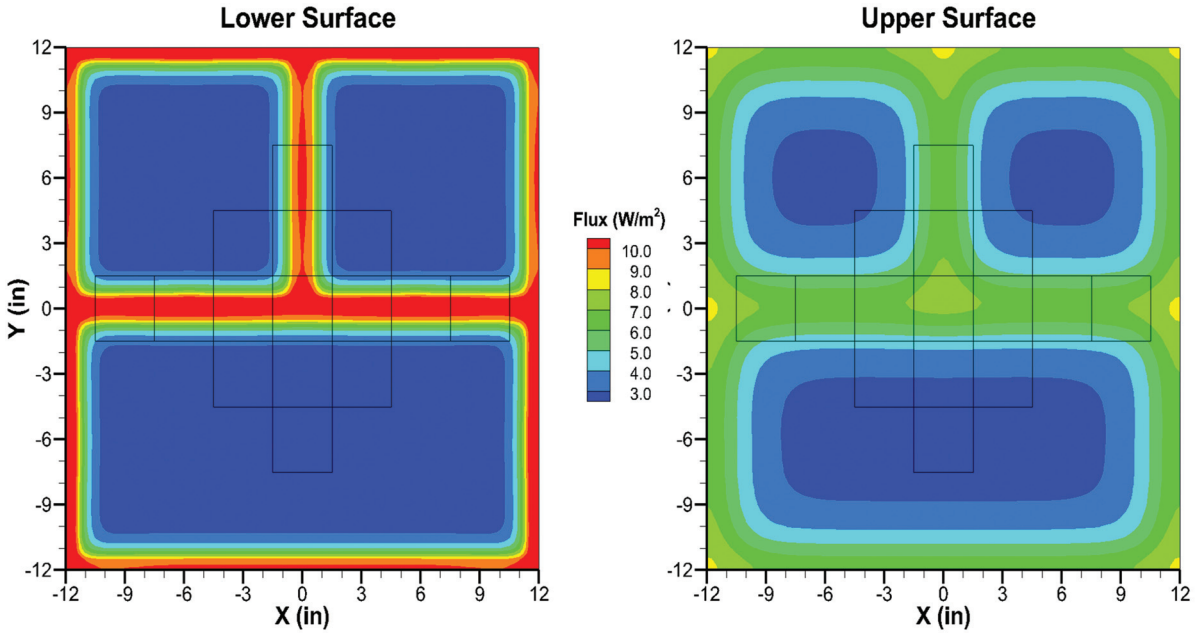

Figure 35 *Calculated flux distributions on lower and upper surfaces: design option 2.*

Since the two transducers nearest the edges of the device (5 and 11) may be influenced by the surroundings (i.e., the edges are not perfectly adiabatic) the optimization was performed two ways: once with all available transducers used and once with edge transducers removed. Removal of transducers 5 and 11 is accomplished by setting their weighting factors to zero. The results for these two optimizations were nearly identical. The calculated and measured heat fluxes are compared for both the upper and lower surfaces of the test specimens, along with contour plots of calculated flux distribution for design options 1 through 4 in Figure 32 to Figure 39.

The resulting properties are given in Table 12. Since some features of the assemblies were not included in the model, the calculated properties may not represent the actual physical properties of the materials, but rather are effective properties that compensate for the impact of the omitted features. Estimated properties from the analyses of design options 1, 2, and 3 are fairly similar to each other: the minimum and maximum estimates of effective core conductivity differ by about 3%. Also, the average calculated value of effective core thermal conductivity matches very well with that found when measuring the center of design option 5, 0.0035 W/m·K, as was shown in Table 12. There is a greater variation in the estimated properties of the barrier material. However, design option 4 produces much lower estimates of the thermal conductivity for both the core material and the barrier. Design option 4 has a band of PVC covering the edges of each of the VIPs and covering the bottom layer of XPS, but not covering the top layer of XPS, as shown in Figure 44. The thermal conductivity of the PVC was obtained from literature values, not measured. It is possible that the value for the PVC conductivity used in the model is too high, resulting in the model predicting lower core and barrier conductivities to compensate. The model assumes that the PVC is in perfect thermal contact with the VIP and the foam insulation—examination of panel after the tests showed that this was not the case. The model also assumes a VIP thickness of 25.4 mm, whereas

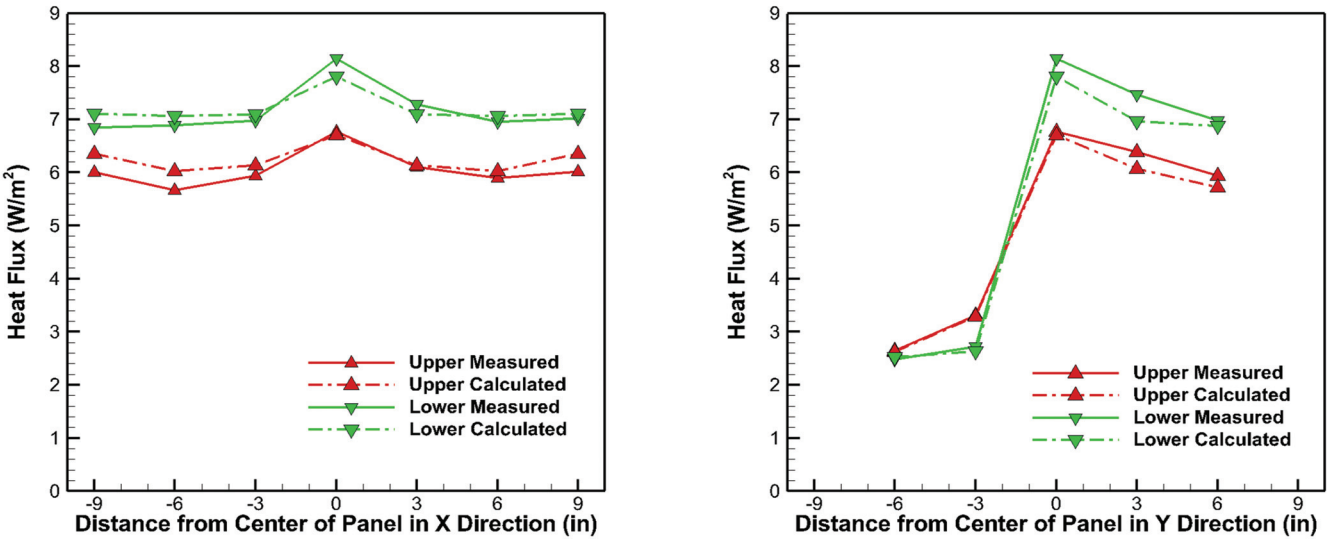

Figure 36 *Measured and calculated fluxes:design option 3.*

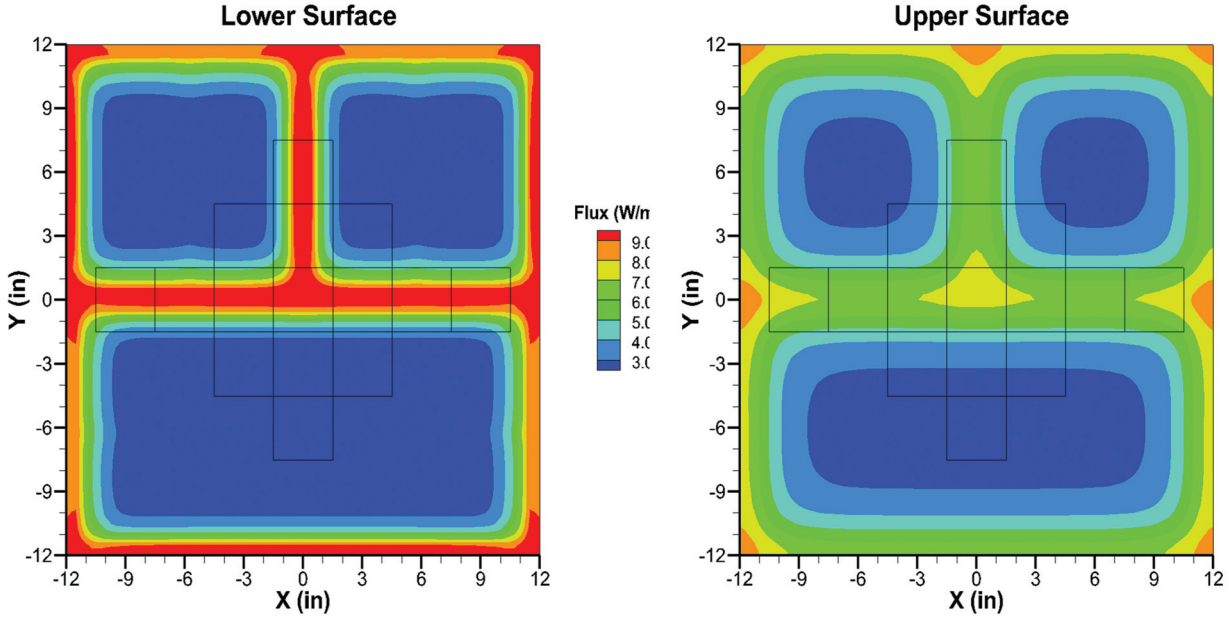

Figure 37 *Calculated flux distributions on lower and upper surfaces: design option 3.*

measurements of two bare VIPs gave values of 26.23 mm and 25.14 mm. The variation in the VIP thickness is on the same order as the variability in the calculated core conductivities for tests on design options 1–3. These factors illustrate the importance of obtaining accurate data as input to a model being used to estimate other parameters. There is greater confidence in the property estimates from design options 1–3.

Earlier studies at ORNL (Wilkes et al. 1997; Wilkes et al. 1999; Stovall and Brzezinski 2002) have indicated that it is difficult to determine the properties of both the core and barrier from testing of the assembly only. The heat flux at any transducer location results from a combination of heat conducted directly through the core and heat conducted around the core in the barrier. An increase/decrease in the core conductivity can be offset by a decrease/increase in barrier conductivity to produce about the same average heat flux at a transducer location. When trying to minimize the difference between the measured and calculated heat fluxes there is not a single, narrowly-defined combination but rather a range of combinations of conductivities that give nearly the same result. The optimizer will find the combination that gives the best fit, but there may be other combinations near this one that are almost as good.

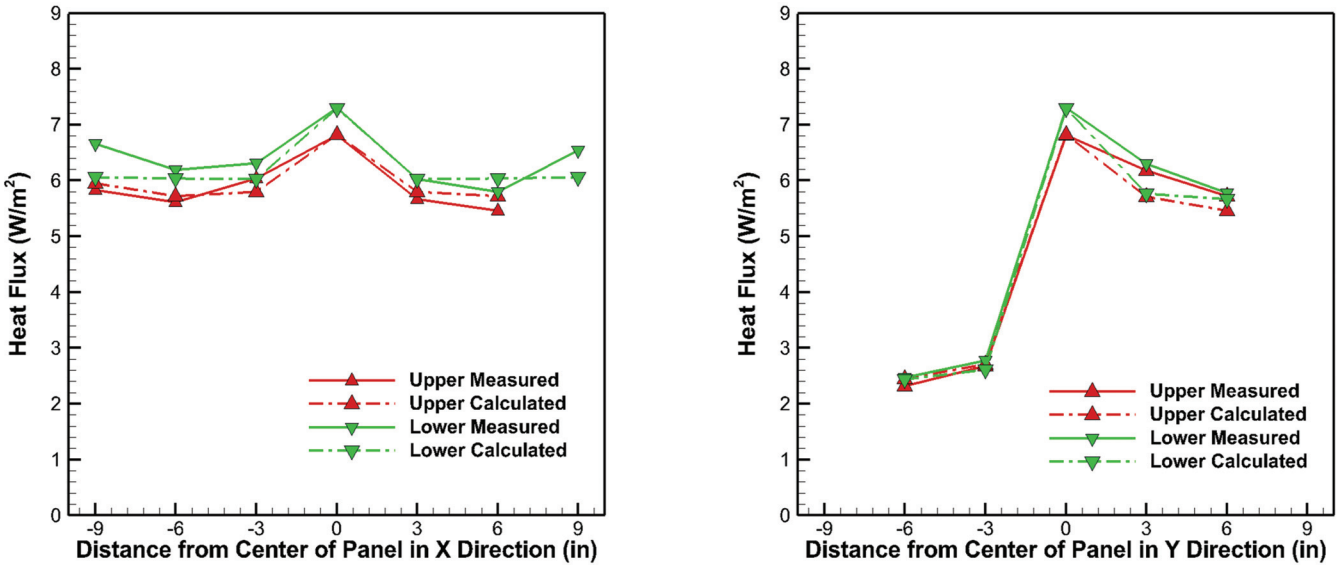

Figure 38 *Measured and calculated fluxes: design option 4.*

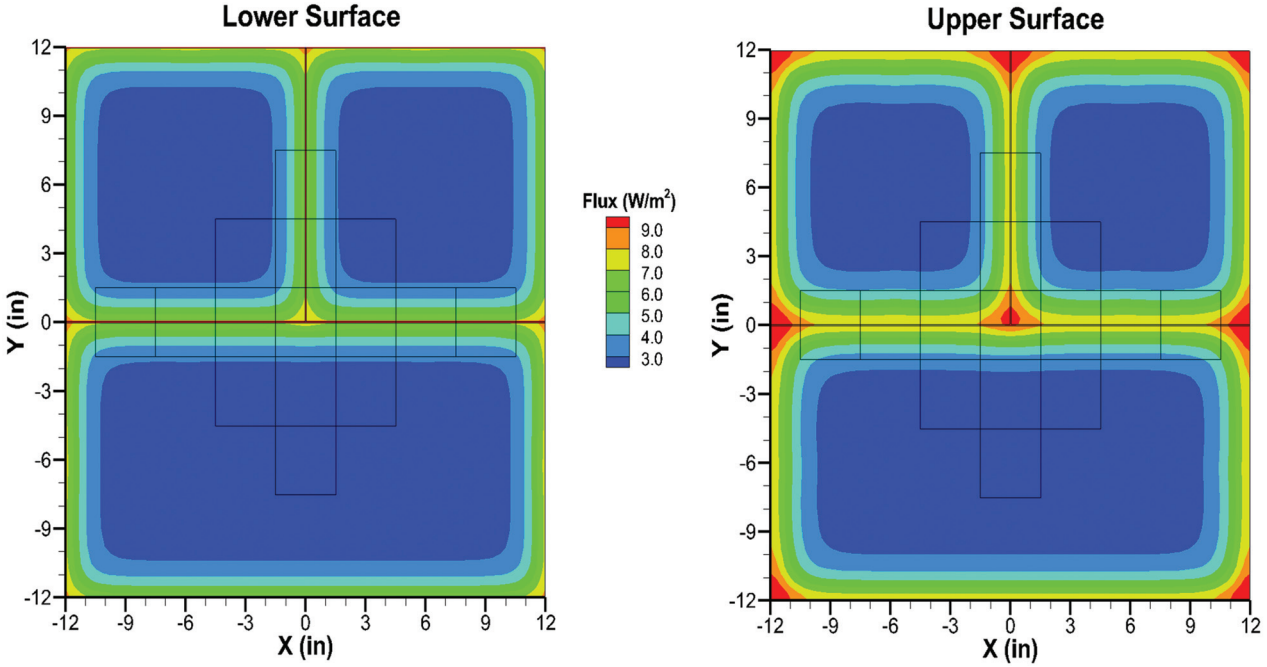

Figure 39 *Calculated flux distributions on lower and upper surfaces: design option 4 (PVC extends from bottom plate to top of VIP, but does not extend upwards to the top plate).*

Since there is an independent measurement of the core thermal conductivity, there might be more confidence in the ability to calculate the barrier properties if the core conductivity is assumed to be fixed. However there would still be a problem with the impact of the features that are not included in the model. With the core conductivity fixed at the value obtained from testing design option 5 (3.50×10^{-3} W/m·K) the barrier conductivity/thickness product was varied to determine the value that gives the best fit to the measured heat flux data. The results of this exercise are given in Figure 41 for design options 1, 2, and 3. This graph shows the optimization function defined in Equation 3 and the results are very similar to those obtained when simultaneously optimizing on both the barrier and core properties, shown in Table 12. Given the uncertainties in heat flux measurement and geometry details, the scatter shown in Table 12 may be indicative of the uncertainty in the calculated properties.

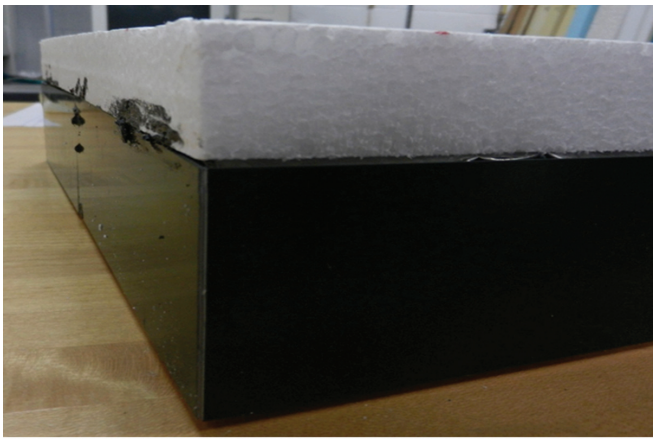

Figure 40 *Corner view of design option 4 test specimen.*

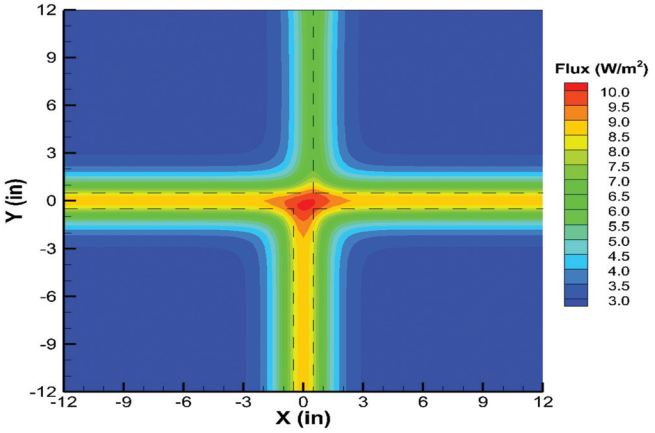

Figure 42 *Surface flux around VIP joints for assembly tested in hot box.*

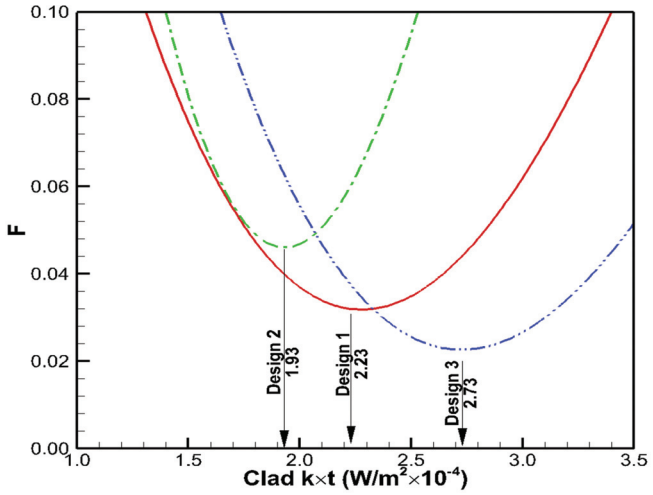

Figure 41 *Optimal clad properties with core conductivity fixed at 0.0035 W/m·K.*

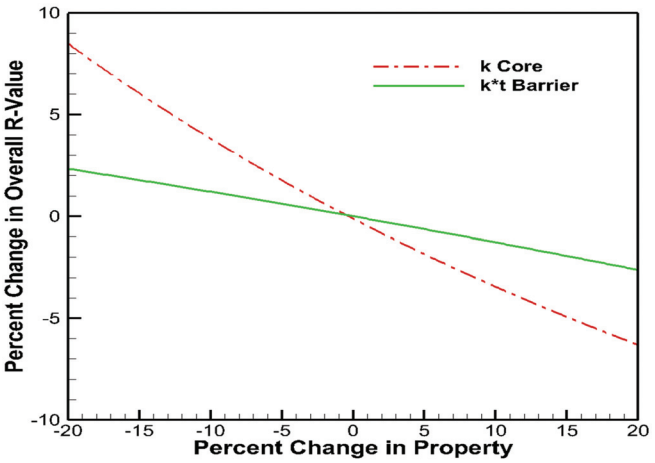

Figure 43 *Sensitivity of R-value to changes in VIP's constituent properties.*

NUMERICAL MODELING OF VIPS

A model was developed of a 24 in.^{2} portion of the VIP assemblies used in the 10 ×10 ft wall tested in the rotatable guarded hot box. This portion is representative of the whole wall because the pattern repeats to cover the entire wall surface. The VIP properties used in the model were those derived from tests of design options 1, 2, and 3, that is 0.00353 W/m^2 for the effective core region thermal conductivity and 0.00023 W/K for the barrier conductance. The same temperature boundary conditions used in the HFM tests were applied to the surfaces. The resulting heat flux is given in the Figure 42. In this figure, the top two vacuum panels are butted against each other, while the bottom two panels are separated by a piece of EPS foam insulation. To achieve this design, the top left vacuum panel is actually slightly larger than the other vacuum panels, as can be seen in the offset between the upper joint parallel to the *y*-axis and the lower joint. This is also reflected in the heat flux map, with a heat flux of about 7 W/m^2 at the butt joint and about 9 W/m^2 at the EPS joint.

The model gives an R-value of 5.79 m^2·K/W (32.9 h·ft^2·°F/Btu) for 24 in.^{2} model. However, if the effective core conductivity is increased to 0.0041 W/m·K (as was measured in tests 9822 and 9825 for the 600 mm^2 [23.5 in.^{2}] VIPs) is used then the R-value is 5.41 m^2·K/W (30.7 h·ft^2·°F/Btu). Since the model only considers the VIP assembly and not the sheathing, stud wall, gypsum board face, and surface film coefficients, the R-value for the wall tested in the hot box would be higher.

Once developed, a model can be used to determine the impact of various factors on the wall's performance. For instance, Figure 43 shows the impact changes in the VIP properties have on the assembly's R-value. The R-value is much more sensitive to changes in the effective core conductivity than it is to changes in the barrier conductivity-thickness product. The model was also used to examine the impact of the barrier

seals that wrap around the ends of a VIP (as previously shown in Figure 32). When the multiple layered areas in the model were changed to a single layer of barrier material the R-value improved by 2.7%.

SUMMARY AND CONCLUSIONS

A proposed wall system incorporates VIPs enclosed within closed-cell insulating foam. In addition to adding some thermal resistance the foam serves to protect the vacuum panels during construction and to provide a surface appropriate for an adhesive joint on both sides of the foam VIP unit.

Multiple configurations of a composite VIP foam insulation structure were evaluated using small sub-sections that could be placed within a HFM apparatus. Through careful test specimen construction, all component joints were located within the range of an array of HFTs installed within the upper and lower plates of that apparatus. Special calibration procedures were used to ensure accurate heat flux measurements for these very-low thermal conductivity specimens. The resulting measurements were combined with modeling efforts to investigate the impact of vacuum-panel size, the type of foam used to encase the vacuum panels, the thickness and shape of the foam sections between panels, and possible adhesive effects.

Some of the proposed configurations placed a greater amount of foam insulation on one side of the VIP panels than on the other. For a given total amount of foam insulation, this arrangement was found to produce a more uniform heat flux, and therefore more uniform temperature distribution, on the outside of the thicker foam surface. This may prove useful if there is any concern with regard to uneven surface soiling phenomena. However, panels constructed in this manner would have the inner and outer faces clearly marked to ensure proper installation during the construction process.

A new procedure was developed to map the HFM measurement results onto full-scale wall designs to predict the system thermal performance. This new method for mapping transducer measurements onto an array of larger panels shows promise, and was used to quantify the expected performance of several candidate construction arrangements. Several potential arrangements of the foam VIP unit were also evaluated using a finite-difference methodology.

The major conclusions of the project can be summarized as:

- It is possible to develop a wall with an overall performance of U-factor of 0.19 W/(m^2·K) (R-30 [h·ft^2·F]/Btu) or greater with multiple VIP arrangements.
- The best arrangements are those that maximize VIP coverage.
- The wall thermal performance is much more sensitive to the effective core thermal conductivity than to the barrier thermal conductance.
- Distributing a greater portion of the foam insulation on the side of the panel facing the exterior environment may be advantageous.

ACKNOWLEDGMENTS

This report was prepared as an account of work sponsored by an agency of the United States Government and Dow Corning. Neither the United States Government, Dow Corning, nor any agency thereof, nor any of their employees, makes any warranty, express or implied, or assumes any legal liability or responsibility for the accuracy, completeness, or usefulness of any information, apparatus, product, or process disclosed, or represents that its use would not infringe privately owned rights. Reference herein to any specific commercial product, process, or service by trade name, trademark, manufacturer, or otherwise, does not necessarily constitute or imply its endorsement, recommendation, or favoring by the United States Government or any agency thereof. The views and opinions of authors expressed herein do not necessarily state or reflect those of the United States Government or any agency thereof.

REFERENCES

ASTM. 2010. ASTM Standard C177, *Standard Test Method for Steady-State Heat Flux Measurements and Thermal Transmission Properties by Means of the Guarded-Hot-Plate Apparatus*. West Conshohocken, PA: ASTM.

ASTM. 2010. ASTM Standand C518, *Standard Test Method for Steady-State Thermal Transmission Properties by Means of the Heat Flow Meter Apparatus*. West Conshohocken, PA: ASTM.

ASTM. 2010. ASTM Standard C1667, *Standard Test Method for Using Heat Flow Meter Apparatus to Measure the Center-of-Panel Thermal Resistivity of Vacuum Panels*. West Conshohocken, PA: ASTM.

Childs, K.W. 1993. *HEATING 7.2 User's Manual*, ORNL/TM-12262. Oak Ridge, Tennessee: Oak Ridge National Laboratory.

Stovall, T.K., Brzezinski, A. 2002. *Vacuum Insulation Round-Robin to Compare Different Methods of Determining Effective Vacuum Insulation Panel Thermal Resistance, Insulation Materials: Testing and Applications,* Fourth Volume STP 1426. A. Desjarlais, ed. West Conshohocken, PA: ASTM.

Taylor, B.N., and Kuyatt, C.E. 1994. Guidelines for evaluating and expressing the uncertainty of NIST measurement results, NIST Technical Note 1297.

US Department of Energy. 2008. *Energy Efficiency Trends in Residential and Commercial Buildings*. http://apps1.eere.energy.gov/buildings/publications/pdfs/corporate/bt_stateindustry.pdf.

Wegger, E. P.J. Bjørn, E. Sveipe, S. Grynning, A. Gustavsen, R. Baetens and J.V. Thue. 2011. Aging effects on thermal properties and service life of vacuum insulation panels. *Journal of Building Physics* 35:128.

Wilkes, K.E., et al. 1997 *Development of Metal-Clad Filled Evacuated Panel Superinsulation*, ORNL/M-5871.

Wilkes, K. E., et al. 1999. *Development of Cladding Materials for Evacuated Panel Superinsulation*, C/ORNL 92-0123.